

## Answers to the reviewers

### Referee 1

*The 2010 cloud experiment at Mt. Schmucke (Germany) was performed with much effort and heavily instrumented with regard to cloudwater collection. This manuscript describes a part of the data set (8 events, inorganic ions and DOC) and highlights three topics: The correlation between cloud concentrations and the liquid water content, the scavenging of substances by the cloud, and the cloud-droplet-size dependent concentrations of substances. Some parameters were measured with high time resolution, as two AMS systems were employed in the field. The results are manifold and described in great detail in this manuscript. The evaluation and interpretation of data was performed carefully yet clearly, results are embedded into the respective literature results. Overall, this is an interesting and precious data set. Although not breathtaking, this manuscript should be published in ACP. Some comments are intended to help the authors clarify some issues before final publication in ACP:*

We thank the reviewer for his or her effort and thoughtful remarks and will reply to all comments in the following.

*page 24320, line 26: Schneider (2015) is not a valid reference. Overall in section “2.2 Interstitial and residual particle sampling”, there is no information about how efficient the separation between cloud droplets and interstitial aerosol is.*

We removed the reference to the not yet submitted work and modified the sentence as follows:

“Details of the AMS measurements will be given in a forthcoming companion paper of this special issue (Schneider et al., in preparation)(Schneider et al., 2015).”

With regard to the separation between cloud droplets and interstitial aerosol: This is given in the Schwarzenböck et al., 2000, reference, where we refer the reader to for more details: Collection efficiency increases from 10% to 90% from approx. 4 to 6  $\mu\text{m}$ .

*page 24321, line 5: Poulain et al. (2015) is not a valid reference. The information of the monitor “for continuous (1 h time resolution) determination of water-soluble inorganic trace gases and particulate ions” is too sparse.*

We removed this reference as well and added additional information on the MARGA system as follows:

“A full description of the instrumental setup will be given in a forthcoming companion paper of this special issue (Poulain et al., in preparation). In brief, a commercial monitor for aerosols and gases (MARGA 1S, Metrohm Applikon, The Netherlands) was used for continuous (1 h time resolution) determination of water-soluble inorganic trace gases and particulate ions. The MARGA operated at a sampling rate of  $1 \text{ m}^3 \text{ h}^{-1}$  and consisted of a  $\text{PM}_{10}$  inlet, a wet rotating denuder absorbing water-soluble gases into deionised water (10 ppm  $\text{H}_2\text{O}_2$  added as biocide), a steam jet aerosol collector to grow and collect aerosol particles, and 2 ion chromatography systems for online cation and anion analysis.”

*page 24322, lines 13-19: What about the stability of  $\text{H}_2\text{O}_2$  and  $\text{S(IV)}$  during cloud water collection? These species may react with each other faster than within one hour, which is the time resolution of the cloudwater collection.*

We agree that this can be a potential artefact, which is, however, difficult to address because it is a function of reactant concentrations and cloud water pH over the time of sampling. Observed concentrations of reactive species at the point of sample preservation can thus be more or less biased depending on actual cloud water conditions. To clarify this, we added the following sentence into section 2.5:

“Concentrations of reactive compounds at the time of sample preservation can be biased due to reactions during the collection period. The extent of such artefacts will depend on reactant concentrations and cloud water pH and cannot easily be estimated.”

*page 24323, line 19: Why three sites, didn't you talk about two sites only so far?*

We haven't introduced the third site, because in this manuscript we don't present data from it. We understand this can be confusing, however, and have therefore changed section 2.3 from “Upwind site aerosol sampling” to “Valley sites aerosol sampling” and modified its beginning as follows:

“Next to the Schmücke in-cloud site, two more valley sites upwind and downwind of the Schmücke were installed during HCCT-2010 to characterise air masses before and after their passage through the clouds.”

In addition, we added this sentence at the end of section 2.3:

“Data from the downwind site has not been used in the present contribution.”

*page 24327, line 6: van Pinxteren et al. (2015) is not a valid reference. As “Concentrations of a large number of organic acids were measured from the bulk cloud water samples”, they need to be reported here. The ion balance (Fig. 2) should be complemented by the measured organic acid anions.*

We removed the reference, but would rather not report the organic acid concentrations in detail in this manuscript. These data will be presented and discussed together with a range of other organics in a forthcoming manuscript. Including them here just for the ion balance would lead to duplicate publication. We agree, however, to give more details on the importance of the organic acids for the ion balance in the text and modified the paragraph as follows:

“Concentrations of a large number of organic acids were measured from the bulk cloud water samples and will be presented elsewhere (van Pinxteren et al., in preparation). Summing up the equivalent concentrations of the most abundant determined acids (formic, acetic, glycolic, oxalic, malonic, succinic, and malic acid) with consideration of their respective dissociation states depending on their  $pK_a$  values and sample pH values gives a range of 5 – 82 (average of 23)  $\mu\text{eq L}^{-1}$ , which explains 6 – 100% (average of 56%) of the inorganic anion deficit. In about 10% of the samples organic acid equivalent concentrations significantly exceeded the anion deficit (up to 255%), likely related to measurement uncertainties and/or non-determined cations. Considering that the DOC fraction likely contains many more than the analytically resolved organic acids, it can be assumed that the missing anions are predominantly organic in nature...”

*Figure 3: Do symbols indicate the maximum concentration (CWL) datapoints?*

The dots indicate data outside  $1.5 \cdot \text{IQR}$ . We realise this information was missing and have now included it into the caption of Figure 3:

“..., whiskers extend to 1.5 IQR (interquartile range), and dots indicate individual data points outside this range.”

*page 24328, lines 19-23: This sentence is awkward and not clear. It may be deleted or, if considered important, be expanded in order to better explain the involved processes and conditions.*

We agree and have deleted the sentence. The paragraph now reads:

“While LWC undoubtedly impacts solute concentrations, the additional variance it introduces to observed concentrations seems to be small, overall, and LWC does not seem to be the main driver in solute concentration differences during this study.”

*page 24329, lines 4-6: The sentence “Also in our dataset, LWC does therefore rather control the range of observable TICs than the actual TIC itself, : : :” is not very clear.*

We agree and have deleted this sentence as well. The modified paragraph now reads:

“Maximum TICs are decreasing, while minimum TICs stay relatively constant with increasing LWC, leading to a range of observed TICs at any given LWC. As one and the same LWC value can result from different cloud microphysical conditions...”

*page 24334, lines 25-29: The authors speculate about the potential role of organic acids in DOC behavior. They probably do know the answer, but do not present it to the readers of this manuscript. This is awkward.*

We have checked our data and can tell that the determined main organic acids during the event discussed here (FCE11.2) explain less than 10% of the inorganic anion deficit. We can therefore not further elucidate the role of organic acids in DOC behaviour here. To indicate this to the reader, we have added the following sentence:

“It is noted that the main organic acids mentioned above explain only less than 10% of the inorganic anion deficit for this event.”

sections 3.4.1 and 3.4.2: Please provide some information about the water volumes collected on the individual stages of the collectors.

We have added 2 figures in the supplemental material, giving water volumes per stage collected with the 3-stage (Fig. S8) and 5-stage collectors (Fig. S24). In addition, we added the following to the beginning of section 3.4.1:

“Volumes of cloud water collected per stage were between 5.9 and 240 ml with typically lowest volumes on the intermediate stage (16-22  $\mu\text{m}$ ) and highest volumes in the smaller or larger size class, depending on the sample (see Figure S8 for details).”

To the beginning of section 3.4.2, the following was added:

“Collected cloud water volumes were from 0.55 to 15 ml, with smallest volumes typically in the 4-10  $\mu\text{m}$  droplet size range and largest ones mostly for droplets  $>30 \mu\text{m}$  (see also Figure S24).”

Wouldn't it make sense (despite all overlap between stages) to present LWC and CWL data as functions of droplet size?

Indeed, we had first prepared the figures this way. We found that readability is compromised, however, because of many overlapping lines and therefore switched to the bar plots.

Tab 4 heading: Replace "> 0.2" by "< 0.2"

Thanks, done.

## Referee 2

*The present manuscript describes the chemical composition of clouds sampled during the HCCT-2010 campaign. It features an impressive dataset in terms of physical and chemical parameters (inorganic ions together with DOC) measured. The cloud sampling is performed using several cloud collectors allowing to analyze the cloud chemical composition as a function of the droplet size. Sampling of the interstitial phase and of the cloud water by the CVI/INT system allows estimating the scavenging of the chemicals by the cloud water. Finally, AMS measurements allow to evaluate the variability of the cloud water composition with a high time resolution. Such analysis of cloud chemistry is very rare and difficult and by themselves worthwhile additions to the scientific literature. The discussion of the results is very detailed but clear and organized in a logical way. Some results like the correlation between LWC and cloud concentrations are expected/traditional. Other approaches are rather novel. For example, the way you connect air masses collected at three campaign sites (connected air flow) is interesting and allows documenting "full cloud events". Factors controlling solute concentrations are more subject to debate since there are so many factors that can explain concentration variability... So certain of your conclusions are more or less speculative...*

*Overall the study is an interesting contribution to atmospheric cloud chemistry and I would support publication of the manuscript while encouraging the authors to consider the following comments.*

We thank the reviewer for his or her comments and helpful remarks and will address all suggestions in the following.

*1- The introduction part is too long and should be reduced. Too many details are present and need to be suppressed for more clarity. Most of the information in the introduction part is even discussed in the results part.*

We agree and have removed two details in the introduction section on the control of solute concentrations, as well as omitted a large part of the discussion on solute concentration size dependencies from the Schell et al. modelling study.

*2- p. 24319, line 12 : you argue that samples are stored at -20\_C until analysis. For H<sub>2</sub>O<sub>2</sub> analysis, this can lead to strong underestimation of the concentration. Indeed, the retention coefficient of H<sub>2</sub>O<sub>2</sub> is below 1 (around 0.3 following Snider et al., 1992). This means that about 1/3 of aqueous H<sub>2</sub>O<sub>2</sub> is retained in the crystal during freezing of the samples.*

Actually, this is one of the reasons why H<sub>2</sub>O<sub>2</sub> was stabilized/preserved immediately after sampling and prior to freezing, as described on P24322 L13-16 in the discussion paper.

3- p. 24321. Please notify the nature of the filters (teflon, nylon?).

The sentence was modified as follows:

“Cloud water from the different samplers was filtered through 0.45 µm syringe filters (IC Acrodisc 13, Polyethersulfone membrane, Pall, Dreieich, Germany) and analysed...”

4- p. 24324. Definitely, I think that CASCC2 bulk samplers are not fitted to collect successive cloud water samples... especially for trace ions. For FCE 1.1 and FCE 13.3, the concentrations of certain chemical compounds should be carefully considered. This leads also to a general comment. To my opinion, CASCC2 sampler concentrates the cloud samples due to the way they collect the water. I know that most of the cloud water collection are performed with this Teflon strands system but I prefer the system where droplets impact on flat surface. This leads to my question. Did you compare you measurements performed on cloud water collected by your various cloud water collectors (CASCC2 vs. 5 stage for example)?

Yes, we have compared both the 3-stage and the 5-stage concentration with the ones observed from the bulk CASCC2 collectors and did not find severe deviations. We didn't include it into the manuscript due to paper size reasons, but we agree that it is interesting information and have therefore now included two figures into the supplemental material showing volume-weighted mean concentrations from the multistage collectors plotted versus corresponding bulk concentrations (Fig. S3 and Fig. S4). In addition, we have changed the title of section 3.2 to “Control samples and collector intercomparison” and added the following paragraph at the end of this section:

“Comparisons of volume-weighted mean concentrations from the multistage collectors with bulk concentrations from the CASCC2 for main cloud water constituents (sulfate, nitrate, ammonium, DOC) are shown in Figure S3 and Figure S4. They reveal generally similar data between the samplers with a tendency of sometimes higher concentrations from the multistage collectors, which was, however, not consistently observed for all constituents and/or cloud events.”

5- p. 24325. Your lowest value for cloud pH (3.6) seems really low. You need high concentration of strong inorganic acids (mainly nitrate and sulfate) to reach this value. If you compare for example with puy de Dôme measurements, you reach a pH value closed to 3.6 with significantly higher concentration of nitrate and sulfate. Please discuss.

A minimum pH of 3.6 does not seem extraordinary low to us, given that polluted air masses e.g. from the Rhine/Main area (Frankfurt/Main) can easily reach the rural Schmücke site. As reported by (Deguillaume et al., 2014), pH can reach even lower values in the polluted regime at Puy de Dôme. It is clear that higher concentrations of acids are needed for a pH in this range, but we would not consider this to be worth adding another discussion to the already quite long manuscript.

6- Conclusion. What is the next step? Modeling investigations to explain the results? Is it feasible with current cloud chemistry models? Please discuss.

The reviewer is right in assuming that the experimental data presented here will be used in our multiphase SPACCIM/CAPRAM model (actually has been used already, but data is not published yet). We have added the following as last bullet point to the conclusions section:

- “The comprehensive dataset obtained during HCCT-2010 will serve as a reference for the further development and evaluation of multiphase models in future studies.”

*Minor comments:*

1- Please add in the table 1, pH values for each FCE.

Table 1 contains general information on the FCEs and is quite loaded already. We have added mean pH values to Figure 1, together with total solute concentrations, as suggested below.

2- Figure 1. Please indicate the total concentrations of measured chemicals for each FCE. This will help the readers.

Good point, done.

*Reference: Snider, J. R., D. C. Montague, and G. Vali : Hydrogen peroxide retention in rime ice, J. Geophys. Res., 97 (D7), 7569–7578, 1992.*

## References

- Deguillaume, L., Charbouillot, T., Joly, M., Vaitilingom, M., Parazols, M., Marinoni, A., Amato, P., Delort, A. M., Vinatier, V., Flossmann, A., Chaumerliac, N., Pichon, J. M., Houdier, S., Laj, P., Sellegri, K., Colomb, A., Brigante, M., and Mailhot, G.: Classification of clouds sampled at the puy de Dôme (France) based on 10 yr of monitoring of their physicochemical properties, *Atmos. Chem. Phys.*, 14, 1485-1506, doi: 10.5194/acp-14-1485-2014, 2014.
- Schneider, J., Mertes, S., van Pinxteren, D., Herrmann, H., and Borrmann, S.: In-situ mass spectrometric analysis of cloud residuals and interstitial aerosol composition on orographic clouds during HCCT-2010: Uptake of nitric acid in cloud droplets, *Atmospheric Chemistry and Physics Discussions*, in preparation, 2015.

1 **Cloud water composition during HCCT-2010: Scavenging**  
2 **efficiencies, solute concentrations, and droplet size**  
3 **dependence of inorganic ions and dissolved organic**  
4 **carbon**

5  
6 **D. van Pinxteren<sup>1</sup>, K.W. Fomba<sup>1</sup>, S. Mertes<sup>1</sup>, K. Müller<sup>1</sup>, G. Spindler<sup>1</sup>, J.**  
7 **Schneider<sup>2</sup>, T. Lee<sup>3\*</sup>, J. Collett<sup>3</sup>, and H. Herrmann<sup>1</sup>**

8 [1] Leibniz-Institut für Troposphärenforschung (TROPOS), Permoserstr. 15, 04318 Leipzig,  
9 Germany

10 [2] Max Planck Institute for Chemistry, Hahn-Meitner-Weg 1, 55128 Mainz, Germany

11 [3] Colorado State University, Department of Atmospheric Science, Fort Collins, CO 80523,  
12 USA

13 \*now at: Hankuk University of Foreign Studies, Department of Environmental Sciences,  
14 Yongin, South Korea

15

16 Correspondence to: H. Herrmann (herrmann@tropos.de)

17

18 Revised version, submitted January 2016

19

20 **Abstract**

21 Cloud water samples were taken in September/October 2010 at Mt. Schmücke in a rural,  
22 forested area in Germany during the Lagrange-type Hill Cap Cloud Thuringia 2010 (HCCT-  
23 2010) cloud experiment. Besides bulk collectors, a 3-stage and a 5-stage collector were  
24 applied and samples were analysed for inorganic ions ( $\text{SO}_4^{2-}$ ,  $\text{NO}_3^-$ ,  $\text{NH}_4^+$ ,  $\text{Cl}^-$ ,  $\text{Na}^+$ ,  $\text{Mg}^{2+}$ ,  
25  $\text{Ca}^{2+}$ ,  $\text{K}^+$ ),  $\text{H}_2\text{O}_2$  (aq), S(IV), and dissolved organic carbon (DOC). Campaign volume-  
26 weighted mean concentrations were 191, 142, and 39  $\mu\text{mol L}^{-1}$  for ammonium, nitrate, and  
27 sulfate, respectively, between 4 and 27  $\mu\text{mol L}^{-1}$  for minor ions, 5.4  $\mu\text{mol L}^{-1}$  for  $\text{H}_2\text{O}_2$  (aq),

28 1.9  $\mu\text{mol L}^{-1}$  for S(IV), and 3.9  $\text{mgC L}^{-1}$  for DOC. The concentrations compare well to more  
29 recent European cloud water data from similar sites. On a mass basis, organic material (as  
30  $\text{DOC} \times 1.8$ ) contributed 20-40% (event means) to total solute concentrations and was found to  
31 have non-negligible impact on cloud water acidity. Relative standard deviations of major ions  
32 were 60-66% for solute concentrations and 52-80% for cloud water loadings (CWLs).  
33 ~~Contrary to some earlier suggestions,~~ The similar variability of solute concentrations and  
34 CWLs together with the results of back trajectory analysis and principal component analysis,  
35 suggests that concentrations in incoming air masses (i.e. air mass history), rather than cloud  
36 liquid water content (LWC) was the main factor controlling bulk solute concentrations at Mt.  
37 Schmücke for the cloud studied. Droplet effective radius was found to be a somewhat better  
38 predictor for cloud water total ionic content (TIC) than LWC, even though no single  
39 explanatory variable can fully describe TIC (or solute concentration) variations in a simple  
40 functional relation due to the complex processes involved. Bulk concentrations typically  
41 agreed within a factor of 2 with co-located measurements of residual particle concentrations  
42 sampled by a counterflow virtual impactor (CV) and analysed by an aerosol mass  
43 spectrometer (AMS), with the deviations being mainly caused by systematic differences and  
44 limitations of the approaches (such as outgassing of dissolved gases during residual particle  
45 sampling). Scavenging efficiencies (SEs) of aerosol constituents were 0.56-0.94, 0.79-0.99,  
46 0.71-0.98, and 0.67-0.92 for  $\text{SO}_4^{2-}$ ,  $\text{NO}_3^-$ ,  $\text{NH}_4^+$ , and DOC, respectively, when calculated as  
47 event means with in-cloud data only. SEs estimated using data from an upwind site were  
48 substantially different in many cases, revealing the impact of gas-phase uptake (for volatile  
49 constituents) and mass losses across Mt. Schmücke likely due to physical processes such as  
50 droplet scavenging by trees and/or entrainment. Drop size-resolved cloud water  
51 concentrations of major ions  $\text{SO}_4^{2-}$ ,  $\text{NO}_3^-$ , and  $\text{NH}_4^+$  revealed two main profiles: decreasing  
52 concentrations with increasing droplet size and “U”-shapes. In contrast, profiles of typical  
53 coarse particle mode minor ions were often increasing with increasing drop size, highlighting  
54 the importance of a species’ particle concentration size distribution for the development of  
55 size-resolved solute concentration patterns. Concentration differences between droplet size  
56 classes were typically  $<2$  for major ions from the 3-stage collector and somewhat more  
57 pronounced from the 5-stage collector, while they were much larger for minor ions. Due to a  
58 better separation of droplet populations, the 5-stage collector was capable of resolving some  
59 features of solute size dependencies not seen in the 3-stage data, especially sharp  
60 concentration increases (up to a factor of 5-10) in the smallest droplets for many solutes.



61

62

## 63 1 Introduction

64 Clouds represent an important part of the atmospheric multiphase system. Uptake of gases,  
65 dissolution of cloud condensation nuclei (CCN) constituents, and chemical reactions lead to  
66 complex compositions of their aqueous phase, which are highly variable in time and space  
67 and droplet size. Knowledge of these compositions and their variability is crucial for  
68 understanding a number of important processes in the atmosphere, including droplet  
69 activation and growth (e.g. Taraniuk et al., 2008; Facchini et al., 1999), formation and  
70 transformation of compounds (e.g. Herrmann et al., 2015; Fahey et al., 2005), production and  
71 consumption of important oxidants (e.g. Whalley et al., 2015; Marinoni et al., 2011), or  
72 transport and deposition of pollutants (e.g. Vet et al., 2014; Fowler et al., 2009). The present  
73 contribution presents results of cloud water chemical composition and related measurements  
74 during the Hill Cap Cloud Thuringia 2010 (HCCT-2010) experiment, performed in autumn  
75 2010 at Mt. Schmücke, Germany. It focuses on the aspects of i) main drivers of bulk cloud  
76 water solute concentrations, ii) scavenging efficiencies of aerosol constituents, and iii) size-  
77 resolved droplet composition, which will be introduced here.

78 Whether and to what extent *solute concentrations are controlled by LWC* has been debated in  
79 the literature. Both Möller et al. (1996) and Elbert et al. (2000) concluded from their studies  
80 that LWC was the main parameter in controlling cloud water total ionic content (TIC) and  
81 that this relationship could be described by a power law function. From a comprehensive  
82 literature survey, Elbert et al. (2000) concluded that at any given site the cloud water loading  
83 (CWL, the product of solute concentrations and LWC) would be a fairly constant value (with  
84 “fairly constant” being interpreted as max / mean ratio < 5). While Möller et al. (1996)  
85 ~~acknowledged that different air pollution situations lead to strong deviations from the average~~  
86 ~~power function, Elbert et al. (2000) generalized their findings to the statement that at any~~  
87 ~~given site the cloud water loading (CWL, the product of solute concentrations and LWC)~~  
88 ~~would be a fairly constant value (with “fairly constant” being interpreted as max/mean ratio <~~  
89 ~~5).~~ In a discussion of this proposition (Kasper-Giebl, 2002; Elbert et al., 2002), Kasper-Giebl  
90 (2002) demonstrated that a constant CWL would imply either constant scavenging  
91 efficiencies and substance concentrations in air, or opposite trends of these two parameters,  
92 neither of which can be generally regarded as true. More recently, Aleksic and Dukett (2010)

93 showed for a very large dataset, that the relationship of TIC ~ LWC cannot be described by a  
94 simple function, but rather by a series of exponential distributions of TIC whose means values  
95 decrease with increasing LWC. These authors as well conclude that CWL is a stochastic  
96 quantity and thus cannot be a constant. ~~In their 12 year dataset of 3300 records, CWL had a~~  
97 ~~relative standard deviation (RSD, standard deviation divided by mean times 100) of 107 %.~~  
98 ~~The RSD of TIC was only slightly larger (127 %), contradicting the earlier conclusions of~~  
99 ~~both Möller et al. (1996) and Elbert et al. (2000) of LWC being the main driver in TIC~~  
100 ~~variability.~~ In section 3.3.2 of this work the parameters controlling bulk cloud water solute  
101 concentrations are studied for the comparatively uniform conditions during HCCT-2010 (with  
102 its identical site, season and wind sector during sampling).

103 *Scavenging efficiencies* (SEs) indicate how much of a compounds' total concentration is  
104 recovered in the cloud liquid phase after cloud formation. Different approaches for its  
105 calculation exist. Cloud water concentrations and interstitial particulate and/or gaseous  
106 concentrations have been used to derive in-cloud scavenging efficiencies of non-volatile or  
107 (semi)-volatile compounds (Sellegri et al., 2003; Acker et al., 2002; Hitzenberger et al., 2000;  
108 Kasper-Giebl et al., 2000; Daum et al., 1984). Alternatively, cloud concentrations can be  
109 related to total particulate (and/or gaseous) concentrations upwind of a cloud (van Pinxteren  
110 et al., 2005; Svenningsson et al., 1997; Leaitch et al., 1986; Hegg et al., 1984) or before  
111 cloud/fog onset (Gilardoni et al., 2014; Collett et al., 2008; Noone et al., 1992). In the ideal  
112 case of a "closed system" with conserved masses, all approaches would lead to the same  
113 scavenging efficiencies. However, as real clouds and fogs are open and dynamic systems,  
114 heavily interacting with their physical and chemical environment, the different approaches  
115 might lead to different results and comparing these might allow for insights into important  
116 processes taking place in the cloud/fog system. In the present study, many (though not all) of  
117 the phases relevant for the concentrations of major cloud constituents (sulfate, nitrate,  
118 ammonium, DOC) have been measured both upwind and inside of clouds at the Schmücke  
119 and are used to calculate and compare scavenging efficiencies derived from different  
120 approaches (section 3.3.4).

121 In clouds, *solute concentrations typically vary across droplet size* (Bator and Collett, 1997;  
122 Rao and Collett, 1995), which has significant implications for chemical reactions in droplets  
123 (Fahey et al., 2005; Reilly et al., 2001; Hoag et al., 1999; Gurciullo and Pandis, 1997) and  
124 deposition behaviour of solutes (Moore et al., 2004b; Collett et al., 2001; Bator and Collett,

125 1997). A conceptual model developed by Ogren et al. (1992) qualitatively describes the  
126 variation of non-volatile solute concentrations with cloud drop size in 3 different drop size  
127 regions: Region I ranges from  $< 1\mu\text{m}$  to approx.  $5\mu\text{m}$  drop diameter (exact size range  
128 strongly depends on cloud properties) and contains freshly activated (or non-activated)  
129 droplets close to their equilibrium size at the prevailing supersaturation. In this so-called  
130 “equilibrium growth” region, solute concentrations sharply decrease with increasing drop  
131 size, because at their critical diameter, larger droplets are more dilute than smaller ones as a  
132 result of the interactions between the Kelvin and the Raoult effect (Pruppacher and Klett,  
133 2010; Ogren and Charlson, 1992). Region II, ranging from approx.  $5 - 50\mu\text{m}$ , represents  
134 droplets which have freely grown by water condensation beyond their critical size. In this  
135 “condensation growth” region, solute concentrations increase with increasing drop size,  
136 because small drops grow faster than large drops ( $r^{-1}$  growth law), i.e. large drops experience  
137 less dilution as compared to smaller ones. In region III, above approx.  $50\mu\text{m}$  in diameter,  
138 coalescence of drops becomes important. As larger drops collide more efficiently with smaller  
139 (i.e. more diluted) ones, solute concentrations decrease with increasing drop size in this  
140 “coalescence growth” region.

141 In more detailed numerical simulations, Schell et al. (1997) studied parameters determining  
142 non-volatile solute concentrations in different droplet sizes. Their results show size  
143 dependencies which are in principle consistent with the three regions in the conceptual model  
144 of Ogren et al. (1992). However, the exact shape of the curve strongly depends on several  
145 parameters, ~~one of them being like~~ the droplet growth time (cloud age), ~~the width of the CCN~~  
146 ~~number distribution (e.g. presence of coarse particles), and the soluble fraction of input~~  
147 ~~aerosol particles. In some cases, the concentration increase in the Ogren et al. region II can~~  
148 ~~diminish to the point of constantly decreasing solute concentrations with increasing droplet~~  
149 ~~sizes nearly over the full droplet size range. In a freshly formed cloud (e.g. a hill cap cloud~~  
150 ~~close to its base), there is a sharp solute concentration increase for droplets with diameters~~  
151 ~~between approx.  $5$  and  $30\mu\text{m}$  (region II in the Ogren et al. model), while for smaller and~~  
152 ~~larger drops concentrations decrease with increasing size (regions I and III). With increasing~~  
153 ~~cloud age (i.e. droplet growth time or height within cloud), however, the rate of concentration~~  
154 ~~increase in region II diminishes, eventually leading to a profile of decreasing solute~~  
155 ~~concentrations with increasing droplet sizes in this drop size range (followed by increasing~~  
156 ~~concentrations for larger drops). A second important parameter was found to be the width of~~  
157 ~~the CCN number distribution, which determines both the drop diameter at the transition point~~

158 ~~from region II to III in the Ogren et al. model (i.e. increasing vs. decreasing solute~~  
159 ~~concentrations with increasing drop size), as well as the maximum solute concentration at this~~  
160 ~~diameter. In simulation runs with narrowed CCN distributions (either by reducing maximum~~  
161 ~~particle diameters in the initial size distributions or by reducing the maximum supersaturation~~  
162 ~~and thus increasing the minimum CCN size limit), the transition between regions II and III~~  
163 ~~was shifted towards smaller drops (diameter  $< 10 \mu\text{m}$  in the extreme case) and the solute~~  
164 ~~concentration at this drop size decreased drastically. Similar to the scenario of an aged cloud,~~  
165 ~~this can lead to constantly decreasing solute concentrations for drop diameters larger than~~  
166 ~~about 5–10  $\mu\text{m}$ . A third parameter influencing solute drop size dependencies was reported to~~  
167 ~~be the soluble fraction of input aerosol particles. While input particles with soluble fractions~~  
168 ~~of 25 and 50 % yielded solute concentration profiles consistent with the Ogren et al. model~~  
169 ~~(including a strong increase of concentrations in region II), solute concentrations deriving~~  
170 ~~from largely insoluble particles (2 % soluble fraction) tended to decrease with increasing drop~~  
171 ~~size nearly over the full drop size range.~~

172 ~~This~~ese ~~discussion of the~~ model results illustrates the complexity of solute concentration drop  
173 size dependencies, which is even increased in reality by many factors such as gas-phase  
174 uptake of soluble material, chemical reactions in droplets, size-dependent composition and  
175 variable mixing state of input aerosol, entrainment processes, and inhomogeneous fields of  
176 supersaturation, i.e. different histories of individual droplets (Flossmann and Wobrock, 2010;  
177 Ogren and Charlson, 1992). In addition, available instrumentation for size-resolved droplet  
178 sampling usually integrates both over extended droplet size ranges with mostly  $\sim 2$  size  
179 fractions only and time periods of typically hours, yielding volume-weighted sample  
180 concentrations which can significantly blur existing concentration gradients (Moore et al.,  
181 2004a, and references therein; Ogren and Charlson, 1992). Despite such difficulties,  
182 observations of size-dependent solute concentrations are still important as available  
183 measurements especially for more than two size fractions are very sparse. In the present  
184 study, a 3-stage and a 5-stage collector were applied and the observed solute concentration  
185 size dependencies are discussed in section 3.4 in view of the above described existing  
186 knowledge.

187

## 188 **2 Materials and methods**

### 189 **2.1 Cloud water sampling**

190 Cloud water sampling took place on top of a 20 m high tower at Mt. Schmücke (Thuringia,  
191 Germany, 50°39'16.5" N, 10°46'8.5" E, 937 m asl) with several collectors. Bulk cloud water  
192 samples were collected into pre-cleaned plastic bottles using the Caltech Active Strand Cloud  
193 Water Collector Version 2 (CASCC2, Demoz et al., 1996), which has a 50% collection  
194 efficiency cut-off diameter ( $D_{50}$ ) of 3.5  $\mu\text{m}$  and collects droplets by inertial impaction on  
195 Teflon strands within the airflow through the instrument. To increase the collected volume of  
196 cloud water for chemical analyses, 4 individual instruments were run in parallel with a time  
197 resolution of one hour. After weighing for volume determination, the samples were pooled,  
198 aliquots for different chemical analyses were taken and aliquots as well as leftover samples  
199 were stored at  $-20^{\circ}\text{C}$  until analysis. For size-resolved droplet sampling a 3-stage collector  
200 (Raja et al., 2008) with nominal  $D_{50}$  of 22, 16, and 4  $\mu\text{m}$  for stages 1, 2, and 3, respectively,  
201 was used. This collector is basically a size-fractionating version of the CASCC, using Teflon  
202 strands/banks with different diameters and different spacing in the 3 stages. In addition, the  
203 CSU 5-stage collector (Moore et al., 2002) with nominal  $D_{50}$  of 30, 25, 15, 10, and 4  $\mu\text{m}$  for  
204 stages 1 – 5 was operated. In contrast to the 3-stage, the 5-stage collector impacts droplets on  
205 flat surfaces downstream of jets with decreasing diameters for air acceleration (cascade  
206 impactor design). It has to be noted, that experimentally determined  $D_{50}$ s for this sampler  
207 differ somewhat from the nominal values and that, even though droplet separating  
208 characteristics have been improved over other existing multistage collectors, there is still  
209 considerable mixing of droplets of different sizes within each stage (Straub and Collett,  
210 2002). Due to limitations of the lateral channel blower applied in this study, the 5-stage  
211 collector was operated about 10% below its nominal air flow rate of  $2.0 \text{ m}^3 \text{ min}^{-1}$ , which  
212 likely had a modest effect on its collection characteristics and adds some uncertainty to the  
213 real cut-off diameters. Sample handling from the multistage collectors was the same as  
214 described for the bulk collectors. Before each cloud event, the samplers were cleaned by  
215 spraying deionised water into the inlet (bulk collectors) or taking apart the individual stages  
216 and rinsing all surfaces with deionised water (multistage collectors). Control samples were  
217 taken after the cleaning procedures by spraying deionised water into the samplers and  
218 handling the collected water in the same way as the real samples.

## 219 **2.2 Interstitial and residual particle sampling**

220 To complement the liquid cloud water samples, droplet residuals and interstitial particles were  
221 sampled downstream of a counter-flow virtual impactor (CVI) and an interstitial inlet (INT).  
222 The CVI/INT system was set up in a building next to the measurement tower with the inlets  
223 installed through a window at 15 m height, facing south-west direction (215°). Details of the  
224 setup can be found elsewhere (Mertes et al., 2005; Schwarzenböck et al., 2000). In brief,  
225 interstitial particles and gases are separated from cloud droplets in the CVI by a counter-flow  
226 air stream which allows only droplets larger 5 µm in diameter to enter the system. Inside the  
227 CVI the droplets are evaporated in particle-free and dry carrier air, resulting in the formation  
228 of dry residual particles consisting of non-volatile cloud water components. Volatile  
229 components can be expected to evaporate during the drying process. The INT inlet samples  
230 interstitial particles and gases by segregating droplets larger 5 µm. Downstream of INT and  
231 CVI, particles were sampled on quartz filters (MK 360, Munktell, Bärenstein, Germany, 47  
232 mm for CVI, 24 mm for INT) with sampling durations typically varying between ca. 4 and 8  
233 hours (some shorter and longer sampling events existed as well). Filters were stored at -20°C  
234 for later offline analysis. Online measurements of submicron particle composition were  
235 performed by two aerosol mass spectrometers (AMS, Aerodyne Research Inc., USA): a C-  
236 TOF-AMS for droplet residuals (CVI, 5 min time resolution) and a HR-TOF-AMS for non-  
237 activated particles (INT, 2.5 min time resolution). Details of the AMS measurements ~~are will~~  
238 be given in a forthcoming companion paper of this special issue (Schneider et al., in  
239 preparation).

## 240 **2.3 Upwind-Valley sites aerosol sampling**

241 Next to the Schmücke in-cloud site, two more valley sites upwind and downwind of the  
242 Schmücke were installed during HCCT-2010 to characterise air masses before and after their  
243 passage through the clouds. Characterisation of incoming aerosol was performed at the  
244 upwind measurement site close to the village of Goldlauter (50°38'15"N, 10°45'14"E, 605 m  
245 asl). A full description of the instrumental setup ~~is will be~~ given in a forthcoming companion  
246 paper of this special issue (Poulain et al., in preparation). In brief, a commercial monitor for  
247 aerosols and gases (MARGA 1S, Metrohm Applikon, The Netherlands) was used for  
248 continuous (1 h time resolution) determination of water-soluble inorganic trace gases and  
249 particulate ions. The MARGA operated at a sampling rate of 1 m<sup>3</sup> h<sup>-1</sup> and consisted of a PM<sub>10</sub>  
250 inlet, a wet rotating denuder absorbing water-soluble gases into deionised water (10 ppm

251 | [H<sub>2</sub>O<sub>2</sub> added as biocide](#)), a steam jet aerosol collector to grow and collect aerosol particles, and  
252 | [2 ion chromatography systems for online cation and anion analysis](#). Size-resolved particle  
253 | sampling was performed using a 5-stage Berner impactor with D<sub>50s</sub> of 0.05, 0.14, 0.42, 1.2,  
254 | 3.5, and 10 μm and a sampling flow rate of 75 l min<sup>-1</sup>. [Data from the downwind site has not](#)  
255 | [been used in the present contribution](#).

## 256 | **2.4 Cloud microphysical and meteorological parameters**

257 | Cloud liquid water content (LWC), droplet surface area (PSA), and effective droplet radius  
258 | (R<sub>eff</sub>) were measured continuously by a particle volume monitor (PVM-100, Gerber  
259 | Scientific, USA), which was mounted on the roof of a building next to the measurement  
260 | tower. Droplet number distributions were obtained from a forward-scattering spectrometer  
261 | probe (FSSP-100, PMS Inc., Boulder, CO, USA), sitting on the top platform of the  
262 | measurement tower. A Ceilometer (CHM15k, Jenoptik, Jena, Germany) was installed at the  
263 | upwind site Goldlauter to derive cloud base heights (CBHs). Standard meteorological  
264 | parameters (temperature, air pressure, relative humidity, wind direction, wind speed, global  
265 | radiation, precipitation) were determined by automatic weather stations (Vantage Pro2, Davis  
266 | Instruments Corp., Hayward, CA, USA) both at the upwind site (ca. 3 m above ground) and  
267 | on the Schmücke measurement tower (ca. 22 m above ground).

## 268 | **2.5 Chemical analyses**

269 | Cloud water from the different samplers was filtered through 0.45 μm syringe filters ([IC](#)  
270 | [Acrodisc 13, Polyethersulfone membrane](#), Pall, Dreieich, Germany) and analysed for  
271 | inorganic ions Cl<sup>-</sup>, NO<sub>3</sub><sup>-</sup>, SO<sub>4</sub><sup>2-</sup>, Na<sup>+</sup>, NH<sub>4</sub><sup>+</sup>, K<sup>+</sup>, Mg<sup>2+</sup>, and Ca<sup>2+</sup> by ion chromatography (IC)  
272 | with conductivity detection (ICS3000, Dionex, Dreieich, Germany). Cation separation was  
273 | performed in a CS16 column (3 mm) applying a methanesulfonic acid eluent, while anions  
274 | were separated using a KOH eluent in an AS18 column (2 mm). Inorganic ions from CVI and  
275 | INT filters were determined by the same method after extraction in deionised water (Milli-Q,  
276 | Millipore, Schwalbach, Germany) and filtration through a 0.45 μm syringe filter. Blank  
277 | correction of filter data took place by subtracting mean concentrations from three unloaded  
278 | field blank filters.

279 | Dissolved organic carbon (DOC) was determined from filtered cloud water samples using a  
280 | TOC-V<sub>CPH</sub> analyser (Shimadzu, Japan) in the NPOC (non-purgeable organic carbon) mode

281 (van Pinxteren et al., 2009). Hydrogen peroxide ( $\text{H}_2\text{O}_2$ ) in solution was determined (in sum  
282 with organic peroxides) by fluorescence spectroscopy (Shimadzu RF-1501) following the  
283 method of Lazrus et al. (1985). To stabilize peroxides during sample storage, p-  
284 hydroxyphenylacetic acid solution (POPHA) was added to aliquots of cloud water  
285 immediately after sampling to form a stable dimer (Rao and Collett, 1995). S(IV) and its  
286 reservoir species hydroxymethanesulphonate (HMS) were determined spectrophotometrically  
287 (Lambda 900, Perkin Elmer, Waltham, MA, USA) by the pararosaniline method (Dasgupta et  
288 al., 1980). Preservation of total S(IV) and HMS took place following the procedure described  
289 by Rao and Collett (1995). Concentrations of reactive compounds at the time of sample  
290 preservation can be biased due to reactions during the collection period. The extent of such  
291 artefacts will depend on reactant concentrations and cloud water pH and cannot easily be  
292 estimated. Cloud water pH was measured immediately after sampling using an MI-410  
293 combination micro-electrode (Microelectrodes, Inc., USA) regularly calibrated at pH 4 and 7.

## 294 **2.6 Data processing and back-trajectory analysis**

295 Cloud water data are presented either as solute concentration ( $\mu\text{mol L}^{-1}$  or  $\text{mg L}^{-1}$ ) or as  
296 CWLs (sometimes also referred to as equivalent air concentrations) in  $\mu\text{g m}^{-3}$ . CWLs are  
297 derived from the solute concentrations by multiplication with the cloud LWC (in  $\text{g m}^{-3}$ ) and  
298 the molar mass of the compound (in  $\text{g mol}^{-1}$ ), where necessary. For comparison of CWLs  
299 between different instruments and/or sites, concentrations were normalised to standard  
300 temperature and pressure (STP: 273 K, 1013 mbar). Ambient temperature during the time of  
301 sampling was used for normalising cloud water collector data, while room temperature was  
302 used for CVI/INT, MARGA, and AMS data (room temp. at time of calibration for the ladder  
303 one). The open-source statistical software R (R Core Team, 2015) including the ggplot2  
304 package (Wickham, 2009) was used for data processing and plotting. Back trajectories were  
305 calculated using the PC version of the HYSPLIT model (Draxler and Rolph, 2003) with  
306 GDAS  $1^\circ$  resolution data from NOAA's Air Resource Laboratory  
307 (<http://ready.arl.noaa.gov/archives.php>). Residence times indices (RTIs) for different land  
308 cover classes (water, natural vegetation, agriculture, urban areas, bare areas) were derived as  
309 proxies for the impacts of typical emissions over these areas on the sampled air masses  
310 following the methodology described by van Pinxteren et al. (2010).

311



## 312 **3 Results and discussion**

### 313 **3.1 Cloud events**

314 Within about 1/3 of the 6 weeks HCCT-2010 campaign Mt. Schmücke was covered in clouds.  
315 Based on the project philosophy of studying aerosol cloud interactions in a Lagrange-type  
316 approach, only those clouds were sampled for which local meteorological parameters (mainly  
317 wind direction) indicated a good possibility of sampling representative air masses at all three  
318 campaign sites (“connected” air flow, see Tilgner et al., 2014) without substantial loss of  
319 material between the sites (non-precipitating clouds only). After the campaign, these events  
320 were thoroughly evaluated regarding the hypothesis of a connected air flow (Tilgner et al.,  
321 2014), leading to the so-called “Full Cloud Events” (FCEs) with conditions appropriate to  
322 compare data from the different sites in a meaningful way. In [Table 1](#) a list of the  
323 FCEs with cloud water samples available is given together with some additional information  
324 on meteorological and cloud microphysical conditions. Note that the numbering of the events  
325 is based on all clouds occurring during HCCT-2010 and is thus non-consecutive. A total of 8  
326 FCEs were sampled, out of which some belonged to the same cloud appearance at Mt.  
327 Schmücke, but were interrupted either by rain or wind direction out of a predefined South-  
328 West corridor (FCE11.2+3 and FCE26.1+2). Two relatively long FCEs occurred with  
329 durations of 15 h, while the other events were shorter with 2 – 7 h durations. Mean LWCs  
330 ranged between 0.15 and 0.37 g m<sup>-3</sup> and were a function of the in-cloud height of the  
331 measurement site (i.e. Schmücke above cloud base, derived from upwind site cloud base  
332 height measurements). Droplet surface areas were 700 – 1400 cm<sup>2</sup> m<sup>-3</sup> on average with  
333 effective droplet radii of about 6 – 9 µm. Mean event temperatures decreased from about 9 °C  
334 for the first FCE to 1 – 2 °C for the last events at the end of the campaign . The numbers of  
335 samples for the different instruments are given in [Table 1](#) as well according to the time  
336 resolutions of the samplers. Overall, meteorological and cloud microphysical conditions were  
337 typical for clouds at Mt. Schmücke during this time of the year. Many more details on  
338 meteorology are given in Tilgner et al. (2014).

### 339 **3.2 Control samples and collector intercomparison**

340 To check for possible contamination, control samples were taken from the cloud water  
341 collectors in between cloud events (section 2.1) indicating a “field blank” value for the  
342 species determined. Concentration levels in these blanks showed clear differences among the

343 three samplers with highest values from the CASCC2 bulk sampler (Figure S1). In contrast to  
344 the two multistage collectors, the CASCC2 was not disassembled for cleaning, which  
345 indicates that the cleaning procedure applied here (spraying deionised water through the  
346 sampler) is less effective in removing leftover traces from previously sampled cloud water (or  
347 its dried residuals if cleaning was not performed directly after the end of the event). Mean  
348 concentration levels in the controls are usually <10% of cloud water concentrations for more  
349 abundant ions (ammonium, nitrate, sulfate), but can make up significant fractions (up to 100%  
350 or even more in individual samples with low concentration) for trace ions (Figure S2). Mean  
351 blank levels of H<sub>2</sub>O<sub>2</sub> and DOC are 25 and 15% of cloud water concentrations on average,  
352 respectively (Figure S2). The amount of carry-over contamination in the controls depends on  
353 concentration levels in the previous sample as well as on the effectiveness of the cleaning  
354 procedure (water volume applied, dried surfaces, etc.) and will likely vary from one event to  
355 another, which hampers a correction of cloud water concentrations by the available blank  
356 data. Carry-over contamination will likely affect the first sample of a new cloud event mainly,  
357 as the inside-surfaces of the CASCC2 are continuously washed by cloud water during  
358 operation and any contamination can be expected to be removed after the first hour of  
359 sampling. In addition, a fraction of the control sample concentrations can be suspected to  
360 form by uptake of gases during control sampling for species like ammonium (from ammonia),  
361 nitrate (from nitric acid), DOC (from water-soluble volatile organic compounds, VOCs), and  
362 especially H<sub>2</sub>O<sub>2</sub>. Cloud water concentrations are thus reported as measured in the following.

363 Comparisons of volume-weighted mean concentrations from the multistage collectors with  
364 bulk concentrations from the CASCC2 for main cloud water constituents (sulfate, nitrate,  
365 ammonium, DOC) are shown in Figure S3 and Figure S4. They reveal generally similar data  
366 between the samplers with a tendency of sometimes higher concentrations from the multistage  
367 collectors, which was, however, not consistently observed for all constituents and/or cloud  
368 events.

### 369 **3.3 Bulk concentrations**

#### 370 **3.3.1 Composition overview**

371 In Table 2 concentrations of inorganic ions, H<sub>2</sub>O<sub>2</sub> (aq), S(IV), HMS, and DOC as well as  
372 cloud water pH are summarised for the events given in Table 1~~Table 1~~. The observed range of  
373 pH-values was from 3.6 to 5.3, with a mean of 4.3. Highest ion concentrations (on a molar

374 basis) were observed for ammonium, followed by nitrate. Sulfate, chloride, and sodium  
375 showed considerably lower concentrations, while potassium, magnesium, and calcium were  
376 lowest. Arithmetic mean concentrations of this study are compared to literature data from  
377 clouds/fogs at other European sites in Table 3. Note that some authors report arithmetic  
378 means, while others report volume-weighted mean concentrations, which are always lower for  
379 a given dataset (see Table 2). Comparability of literature pH data is even more hampered as it  
380 is either reported as arithmetic mean or derived from either arithmetic or volume-weighted  
381 mean  $H^+$  concentrations (the first approach leading to higher values than the other ones). In  
382 general, however, concentration levels in the present study are often similar to those observed  
383 in more recent campaigns at Puy de Dôme (continental non-polluted regime, Deguillaume et  
384 al., 2014), in the Western Sudety Mountains (Blas et al., 2008), and at the Schmücke site in a  
385 previous campaign (Brüggemann et al., 2005). In contrast, data from the 1980s and 1990s  
386 often show much higher concentrations of sulfate and nitrate (Bridges et al., 2002; Herckes et  
387 al., 2002; Wrzesinsky and Klemm, 2000; Acker et al., 1998; Joos and Baltensperger, 1991;  
388 Lammel and Metzger, 1991), presumably due to the decline in European emissions of  $NO_x$  and  
389  $SO_2$  over the past decades (EEA, 2014). Concentrations of DOC are more sparsely available  
390 in the literature for European clouds. Mean values during HCCT-2010 compare well with data  
391 from Puy de Dôme (continental non-polluted regime, Deguillaume et al., 2014), Rax (Löflund  
392 et al., 2002) and Schmücke (Brüggemann et al., 2005). Data for  $H_2O_2(aq)$  and S(IV) are even  
393 more sparse. In the present study,  $H_2O_2(aq)$  has been found to be within the same order of  
394 magnitude as determined in similar environments (Deguillaume et al., 2014; Brüggemann et  
395 al., 2005; Löflund et al., 2002), while S(IV) is at the lower end of reported concentrations.

396 Average relative compositions based on volume-weighted mean concentrations (in  $mg L^{-1}$ )  
397 are shown in Figure 1 for the main cloud events. DOC was converted to DOM (dissolved  
398 organic matter) using a conversion factor of 1.8 as in previous studies (Giulianelli et al., 2014;  
399 Benedict et al., 2012; Straub et al., 2012; Collett et al., 2008). Solute concentrations are  
400 always dominated by the main ions sulfate, nitrate, and ammonium, explaining approx. 60-  
401 70 % of total determined concentrations (campaign average 62 %). Among them, nitrate  
402 represents the dominant species (approx. 30-50 % of total concentrations, average 35 %),  
403 while sulfate and ammonium comprise lower fractions of total solutes (averages of 14 and 13  
404 %, respectively). Organic compounds contribute approx. 20-40 % (average 28 %) and are thus  
405 another main constituent of cloud water dissolved material. These fractions are similar to  
406 what has been reported for background and anthropogenic influenced conditions at Puy de

407 Dôme (Marinoni et al., 2004) and are – despite the different environment – strikingly similar  
408 to the 20-year mean composition of Po valley fogs with 35 %, 15 %, 18 %, and 25 %  
409 contributions of nitrate, sulfate, ammonium, and DOM, respectively (Giulianelli et al., 2014).

410 The ion balance of inorganic anions versus cations (including  $[H^+]$ ) is shown in [Figure](#)  
411 ~~2~~[Figure 2](#). An anion deficit is observed for nearly all samples, ranging up to  $178 \mu\text{eq L}^{-1}$ .  
412 Inorganic anions missing from the calculation are unlikely to explain the deficit, as they will  
413 have a small impact on the ion balance only (bicarbonate  $< 1 \mu\text{M}$  for given pH values,  
414 bisulfite  $< 3.2 \mu\text{M}$  based on S(IV) and HMS data). Concentrations of a large number of  
415 organic acids were measured from the bulk cloud water samples and will be presented  
416 elsewhere (van Pinxteren et al., in preparation). Summing up the equivalent concentrations of  
417 the most abundant determined acids (formic, acetic, glycolic, oxalic, malonic, succinic, and  
418 malic acid) with consideration of their respective dissociation states depending on their  $pK_a$   
419 values and sample pH values gives a range of 5 – 82 (average of 23)  $\mu\text{eq L}^{-1}$ , which explains 6  
420 – 100% (average of 56%) of the inorganic anion deficit. In about 10% of the samples organic  
421 acid equivalent concentrations significantly exceeded the anion deficit (up to 255%), likely  
422 related to measurement uncertainties and/or non-determined cations. amounting to 3 – 115  
423  ~~$\mu\text{eq L}^{-1}$  and can thus explain a large fraction of the anion deficit.~~ Considering that the DOC  
424 fraction likely contains many more than the analytically resolved organic acids, it can be  
425 assumed that the missing anions are predominantly organic in nature and that organic acidic  
426 material had a non-negligible impact on the cloud water acidity during HCCT-2010. Similar  
427 observations have been made before in other cloud/fog systems (Straub et al., 2012; Hegg et  
428 al., 2002; Khwaja, 1995; Collett et al., 1989).

429

### 430 3.3.2 Factors controlling solute concentrations

431 In [Figure 3](#)~~Figure 3~~[Figure 3a](#) the variability of observed solute concentrations for selected ions is  
432 indicated in box-plots. Variability was high both within events (max/min ratios of up to 5-8  
433 for main ions during the longer events, and up to 5-34 for minor ions), as well as in-between  
434 events (max/min ratios of median conc. between 3 and 6 for main ions, 6-29 for minor ions).  
435 In general, cloud water solute concentration variability can be caused by i) changes in  
436 microphysical cloud conditions, e.g. supersaturation and LWC, ii) changes in CCN  
437 concentration, size distribution, and chemical composition, iii) changes in gas-phase

438 concentrations of soluble gases and corresponding phase equilibria, and iv) chemical reactions  
439 in the cloud water. Distinctly different concentration patterns can be observed in [Figure](#)  
440 ~~3~~[Figure 3a](#) for three ion groups from similar sources, i.e. secondary ions ammonium, nitrate,  
441 and sulfate, sea-salt ions sodium and chloride, and the biomass burning and/or soil marker  
442 potassium, indicating a dominant influence of air mass history and thus CCN concentration  
443 and composition on cloud water solute concentrations. This is most obvious for sodium and  
444 chloride, which show highest concentrations during FCEs 1.1, 22.1, and 26.1+2. During these  
445 events, back-trajectory analysis revealed a stronger influence of marine emissions (residence  
446 time indices above water surfaces were between 0.3 and 0.5, as compared to < 0.2 for the  
447 remaining events, cf. [Figure S35](#)).

448 To remove any influence of LWC fluctuations, CWLs are plotted in [Figure 3](#)~~Figure 3b~~. The  
449 CWL patterns resemble those of solute concentrations to a large extent, suggesting that for  
450 our dataset CCN composition and concentrations of soluble gases (i.e. air mass history) have  
451 a stronger impact on cloud water solute concentrations than LWC variability. Relative  
452 standard deviations (RSDs) of solute concentrations (whole campaign) are 66 %, 60 %, and  
453 60 % for sulfate, nitrate, and ammonium, respectively, and 84-125% for trace ions. RSDs of  
454 CWLs are similar, sometimes even higher, with values of 80 %, 52 %, and 66 % for sulfate,  
455 nitrate, and ammonium, respectively, and 62-96 % for trace ions. Removing LWC variability,  
456 thus, does not reduce concentration variability, at least for the LWC range in this study. This  
457 is similar to ~~the~~ observations of Aleksic and Dukett (2010) from ~~their a~~ much larger dataset  
458 and indicates that LWC is obviously an important, but not necessarily the primary control  
459 factor of solute concentrations. ~~(cf. section 1), and challenges the proposition of CWL~~  
460 ~~generally being a more appropriate measure for pollution characterisation and site~~  
461 ~~comparisons in cloud studies (Elbert et al., 2000, section 1).~~

462 ~~While LWC undoubtedly impacts solute concentrations, the additional variance it introduces~~  
463 ~~to observed concentrations seems to be small, if present at all. This might be either due to~~  
464 ~~effects such as enhanced gas phase uptake or smaller activation diameter, which can be~~  
465 ~~(indirectly) linked to LWC and might counteract the additional variance and/or due to much~~  
466 ~~larger variance in total aerosol concentrations in the air masses the clouds are forming in. In~~  
467 ~~any case, LWC does not seem to be the main driver in solute concentration differences during~~  
468 ~~this study.~~

469 If at all, an inverse functional relationship between solute concentration and LWC (Elbert et  
470 al., 2000; Möller et al., 1996) can only be observed during single events (i.e. when CCN  
471 concentration and composition as well as gas phase concentrations might be regarded  
472 comparably constant) in our dataset. This is shown in ~~Figure 4~~Figure 4a for TIC versus LWC  
473 where the color-coded single event data indicates more or less constantly decreasing TIC with  
474 increasing LWC for some events. Overall, however, the pattern approximates those observed  
475 for larger datasets (Aleksic and Dukett, 2010; Kasper-Giebl, 2002; Möller et al., 1996):  
476 Maximum TICs are decreasing, while minimum TICs stay relatively constant with increasing  
477 LWC, ~~leading to a range of observed TICs at any given LWC.~~ ~~Also in our dataset, LWC does~~  
478 ~~therefore rather control the range of observable TICs than the actual TIC itself, with larger~~  
479 ~~ranges and larger mean values at lower LWC (Aleksic and Dukett, 2010).~~ ~~Given that  $A_s$~~  one  
480 and the same LWC value can result from different cloud microphysical conditions (e.g. few  
481 large drops vs. more small drops) and clouds with similar LWC can form in very different air  
482 masses, this is actually an expected observation. In several other cloud/fog studies  
483 relationships between TIC and/or solute concentrations with LWC were reported to be non-  
484 existent, neither (Giulianelli et al., 2014; Straub et al., 2012; Marinoni et al., 2004; Kasper-  
485 Giebl, 2002).

486 The reason for this ostensible contradiction to the conclusions of the studies by Möller et al.  
487 (1996) and Elbert et al. (2000) might lie in different assessments of the quality of fitted  
488 models. Möller et al. (1996) and Elbert et al. (2000) report power law fits with coefficients of  
489 determination ( $R^2$ ) of 0.27 and 0.38, respectively. Even when considering these values  
490 satisfactory (on the general usefulness of  $R^2$  especially for goodness-of-fit of nonlinear  
491 models see Spiess and Neumeyer (2010)), the presented scatter plots leave room for  
492 questioning the ability of the fitted functions to adequately represent the data.

493 Instead of LWC, Marinoni et al. (2004) report TIC in cloud water at Puy de Dôme to be a  
494 power function of effective droplet radius ( $R_{\text{eff}}$ ), even though with similarly poor  $R^2$  of 0.29.  
495 In ~~Figure 4~~Figure 4b, TIC during HCCT-2010 is plotted against  $R_{\text{eff}}$ , which was determined  
496 by the PVM as well. In contrast to LWC, both maximum and minimum ~~LWC-TIC~~ values are  
497 decreasing with increasing  $R_{\text{eff}}$  in this plot and the relationship comes indeed closer to a  
498 functional one (best fit for simple linear regression;  $R^2$  increases from 0.14 with LWC to 0.52  
499 with  $R_{\text{eff}}$  as explanatory variable). There is, however, still substantial unexplained TIC

500 variation, likely arising from different broadness and/or skewness of the droplet size spectrum  
501 and from processes like phase equilibria and/or aqueous phase reactions.

502 In ~~Figure 4c~~ and ~~Figure 4d~~ the relationships of DOC with LWC and  $R_{\text{eff}}$  are  
503 shown, which are very similar to the ones observed for TIC. Herckes et al. (2013) examine  
504 total organic carbon (TOC) concentrations against LWC for a number of different sites  
505 worldwide. A simple relationship explaining the variation across all locations could not be  
506 identified by the authors. However, their plot looks remarkably similar to the plots of TIC vs.  
507 LWC from the larger datasets referenced above (decreasing spread of concentrations with  
508 increasing LWC), indicating that the main factors controlling the organic content of fog and  
509 cloud water are the same as the ones determining inorganic ion concentrations (likely  
510 nucleation scavenging and some additional gas phase uptake).

511 As a further means to study the various influences on solute concentrations, principal  
512 component analysis (PCA) was performed on cloud water solute concentrations and pH, back  
513 trajectory RTIs, LWC, and  $R_{\text{eff}}$ . Factor loadings of 4 extracted principal components after  
514 Varimax rotation are shown in Table 4. The first factor is highly correlated to air mass  
515 residence times above the oceans and cloud water concentrations of sea-salt constituents  
516 sodium, magnesium, and chloride. The second factor shows high loadings for all 4 main cloud  
517 water solutes (sulfate, nitrate, ammonium, DOC), representing typical main particulate  
518 components in aged continental air masses. The third factor is highly correlated to potassium  
519 and calcium concentrations and air mass residence times above agricultural lands and likely  
520 represents a mixed soil/biomass burning influence. The fourth factor mainly includes the  
521 variability of air mass residence times above urban areas, with no strong correlation to cloud  
522 water constituents. pH shows a weak anticorrelation to this factor, which could indicate an  
523 impact of acidic pollutants in comparably fresh air masses.

524 LWC has a much smaller impact on the marine factor than air mass residence time above  
525 water and its loading on factor 2 is weak as well (in contrast to  $R_{\text{eff}}$ , which has a significant  
526 impact on this factor). This further supports the conclusion of LWC variability impacting  
527 solute concentrations to a lesser extent if several clouds with different air mass histories are  
528 considered.

529 In summary, the discussion in this section shows that no single factor is available to  
530 adequately describe the complex processes controlling solute concentrations of both inorganic  
531 and organic material in bulk cloud water. If a simple functional relationship is needed,  $R_{\text{eff}}$

532 might be a somewhat better choice than LWC. The probabilistic approach of Aleksic,  
533 however, seems more appropriate: For any given LWC (and probably  $R_{\text{eff}}$  as well), solute  
534 concentrations exhibit a (non-linear) distribution, as they depend on several other variables at  
535 the same time.

### 536 3.3.3 Comparison of bulk vs. CVI concentrations

537 In parallel to the bulk cloud water sampling, a CVI separated droplets from the interstitial  
538 phase and enabled the chemical characterisation of residual particles from filters and online  
539 with an AMS (section 2.2). The resulting CWLs of main solutes (normalised to standard  
540 conditions) are compared to the ones obtained from bulk cloud water samples in Figure 5. As  
541 can be seen, the temporal trends are often similar from both time-resolving samplers  
542 (CASCC2 and CVI-AMS), while absolute values can differ. During FCEs 11.3, 22.1, and  
543 26.1+2, the ratios between CASCC2 and CVI-AMS CWLs are close to 1, especially for  
544 ammonium and sulfate (see Figure S46 for ranges of CWL ratios). During FCEs 1.1, 11.2,  
545 and 13.3, this ratio is close to 2 (median), while it can be even higher for nitrate. Time-  
546 integrated mean CWLs from CVI filters are mostly close to the values from the CVI-AMS for  
547 sulfate and nitrate (with the exception of FCE1.1), while for ammonium, they are  
548 substantially lower during 4 out of the 6 events shown. CWL deviations for DOC (for residual  
549 particle data calculated as AMS organics divided by a conversion factor of 1.8 as above) tend  
550 to be lower than for the ions and CASCC2/CVI-AMS ratios are even below 1 during FCEs  
551 1.1, 11.2, and 26.1+2 (Figure S46). DOC CWLs from CVI filters are not given due to  
552 unreliable data from the small masses sampled on the filters.

553 Possible reasons for these deviations are manifold and include i) different sampling locations  
554 in the cloud (tower versus inlet at house wall), ii) different cut-off and detection  
555 characteristics (all dissolved bulk material analysed from CASCC2, while AMS measures  
556 non-refractory submicron residual particles only), iii) different assumptions/corrections for  
557 sampling efficiency (assumption of constant sampling efficiency across droplet size spectrum  
558 for CASCC2, correction of CVI sampling efficiencies based on particle number size  
559 distributions), iv) measurement uncertainties of analytical methods, AMS, and PVM for LWC  
560 measurement, v) – for DOC – uncertainty in the OM to OC conversion factor (1.8) and  
561 inclusion of undissolved organic matter in the AMS residual organics concentration, vi) – for  
562 filter samples – potential negative artifacts from evaporation of semi-volatile particle  
563 constituents during sampling as well as uncertainty from blank correction especially for short



564 sampling times and low sampled masses, and vii) – very important for some species -  
 565 different droplet “pretreatment”, i.e. liquid collection in the bulk sampler versus evaporation  
 566 of water and volatile constituents such as ammonia, nitric acid and dissolved VOCs in the  
 567 CVI. Given all these uncertainties and systematic differences, a general agreement between  
 568 CWLs obtained from the different samplers within a factor of 2 appears well acceptable. A  
 569 notable exception with much less agreement is nitrate during FCE11.2, where bulk cloud  
 570 water CWLs are about a factor of 3.5 higher than CVI concentrations. The reason for the large  
 571 deviation during this event is likely an enhanced concentration of nitric acid, which is taken  
 572 up as nitrate into the bulk cloud water, but can be (partly) released back to the gas phase  
 573 during droplet drying in the CVI (see also the following section).

### 574 3.3.4 Scavenging efficiencies

575 Scavenging efficiencies (SEs) were calculated by two different approaches. “In-cloud SEs”  
 576 are based on cloud water loadings and interstitial particle concentrations (both being  
 577 normalised to STP) and are calculated as follows:

$$578 \quad SE_{in-cloud} = \frac{CWL}{CWL+c_{int}} \quad \text{(Equation 1)}$$

579 with  $SE_{in-cloud}$ : in-cloud scavenging efficiency

580  $CWL$ : cloud water loading in  $\mu\text{g m}^{-3}$ , either from bulk cloud water (CASCC2) or from  
 581 droplet residual concentrations (CVI-AMS and CVI-Filter)

582  $c_{int}$ : interstitial particle concentration in  $\mu\text{g m}^{-3}$  (INT-AMS or INT-Filter)

583 “Upwind SEs”, in contrast, are based on a comparison of STP normalised CWLs and upwind  
 584 concentrations, calculated as:

$$585 \quad SE_{upwind} = \frac{CWL}{c_{upw}} \quad \text{(Equation 2)}$$

586 with  $SE_{upwind}$ : upwind scavenging efficiency

587  $CWL$ : cloud water loading in  $\mu\text{g m}^{-3}$  from bulk cloud water (CASCC2)

588  $c_{upw}$ : upwind concentration from MARGA measurements in  $\mu\text{g m}^{-3}$ , either particulate  
 589 only or total aerosol (particulate + gaseous concentration)

590 | The results of these calculations are shown in [Figure 6](#). In-cloud SEs calculated from  
 591 | the different samplers usually agree well except for cases where sampler intercomparison was

592 poor (section 3.3.3). Comparison with upwind SEs, however, reveals substantial differences,  
593 | which are summarised as event means in [Table 5Table-5](#) (for residual in-cloud SEs only the  
594 | ones based on CVI/INT AMS data are given here to avoid redundancy). Mean in-cloud SEs  
595 | for sulfate are usually  $\geq 0.9$  except for FCE11.2 and FCE13.3, where substantial fractions  
596 | (21-44%, depending on data used) of in-cloud sulfate reside in interstitial particles. During  
597 | these events particle activation curves obtained from comparing measured particle number  
598 | size distributions upwind and in-cloud were comparably shallow and the critical activation  
599 | diameter was larger than during other events (Figure [S75](#)), consistent with larger fractions of  
600 | submicron sulfate not being activated to cloud droplets due to cloud microphysical conditions.  
601 | Consistent with our data, in-cloud SEs of sulfate between 0.52 and 0.99 have been reported  
602 | for clouds at Puy de Dôme, Brocken, and Mt. Sonnblick (Sellegri, 2003; Acker et al., 2002;  
603 | Hitznerberger et al., 2000; Kasper-Giebl et al., 2000), with larger values being more typical.

604 | In contrast to in-cloud SEs, sulfate upwind SEs were mostly  $\ll 0.9$ , indicating incomplete  
605 | mass conservation between the sites. From previous studies at the Schmücke (Brüggemann et  
606 | al., 2005; Herrmann et al., 2005) and results on aerosol processing presented in a forthcoming  
607 | companion paper, it is known that various physical loss processes, such as scavenging of  
608 | cloud droplets by trees and/or entrainment of cleaner air masses from aloft can reduce  
609 | observed concentrations of all particle constituents along the air path from upwind via  
610 | Schmücke towards the downwind site. Upwind SEs being smaller than in-cloud SEs support  
611 | these conclusions of physical particulate mass losses from the upwind to the in-cloud site.  
612 | Only during FCE13.3 upwind SEs are found to be higher than in-cloud SEs, indicating  
613 | additional sulfate mass within the cloud, which could result from chemical production, uptake  
614 | of gaseous  $\text{H}_2\text{SO}_4$  (Roth et al., 2016; Harris et al., 2014; Harris et al., 2013) and/or other  
615 | processes (e.g. entrainment). Similar to sulfate, ammonium shows in-cloud SEs typically  $>$   
616 | 0.9, except for FCE13.3 (large activation diameter). Upwind SEs are similarly large if upwind  
617 | particulate ammonium concentrations are considered only, but drop to mean values between  
618 | 0.4 and 0.7 if gaseous upwind ammonia - which is likely to be taken up by the cloud water at  
619 | least partially- is included in the balance. Consistent with the conclusions from sulfate, the  
620 | lower overall upwind SEs thus likely reflect the impact of physical loss processes at the sites.

621 | For nitrate and DOC, these comparisons look different. While in-cloud SEs are again  $> 0.9$  in  
622 | most cases, upwind SEs are  $> 1$  in most cases, indicating additional nitrate and DOC at the in-  
623 | cloud site (note that event mean DOC upwind SEs in [Table 5Table-5](#) were calculated using

624 water-soluble organic carbon concentrations from impactor samples, as the MARGA analyses  
625 inorganic ions only). For DOC, this most likely results from uptake of water-soluble VOCs  
626 (e.g. acids, aldehydes, ketones) into cloud droplets. The highest value was observed for  
627 FCE11.2, where the inorganic anion deficit was highest as well (Figure 2), indicating  
628 that a significant amount of organic material taken up from the gas-phase must have been  
629 acidic or – alternatively – neutral compounds were oxidised to organic acids upon dissolution  
630 in the cloud droplets. It is noted that the main organic acids mentioned above explain only  
631 less than 10% of the inorganic anion deficit for this event.

632 For nitrate, upwind SEs stay similarly high or even higher than in-cloud SEs even after  
633 considering any upwind HNO<sub>3</sub> measured by the MARGA. Especially when considering that  
634 nitrate likely experiences similar physical mass losses as ammonium and sulfate (which  
635 typically were on the order of 10 – 40% at the downwind site, data not shown here), this  
636 would imply a nitrate budget at the cloud site substantially larger than the sum of particulate  
637 and gaseous nitrate at the upwind site. Given that aqueous phase oxidation of NO<sub>x</sub> to nitrate  
638 can be considered negligible (Seinfeld and Pandis, 2006) and a potential positive nitrate  
639 artefact from hydrolysis of N<sub>2</sub>O<sub>5</sub> in the cloud water can be assumed to be present in similar  
640 magnitude in the wet rotating denuder samples of the MARGA system (Phillips et al., 2013),  
641 such a large budget increase of nitrate at the cloud site seems unrealistic. In addition, a  
642 comprehensive data analysis focussing on aerosol processing during FCEs (manuscript in  
643 preparation) does not yield indications for increased nitrate at a site downwind of the cloud,  
644 neither on average over all FCEs, nor specifically during FCE11.2, where nitrate enrichment  
645 was highest. Any additional nitrate in the cloud water thus needs to evaporate back to the gas  
646 phase upon cloud dissipation.

647 The most likely explanation for the observed discrepancy is a severe underestimation of nitric  
648 acid by the MARGA system. Accurate nitric acid determination is known to be challenging  
649 due to the “stickiness” of the molecule (Rumsey et al., 2014) and adsorption in the inlet was  
650 reported to be strongly increased when sampling air – as during FCE sampling - is near 100%  
651 RH (Neuman et al., 1999). As the inlet HDPE tubing during HCCT-2010 was approx. 3.5 m  
652 long (from PM<sub>10</sub> head to denuder), significant losses of HNO<sub>3</sub> before denuder sampling seem  
653 likely. In a not (yet) published intercomparison of nitric acid between the MARGA unit as  
654 used during HCCT-2010 and a separate batch denuder with inlet tubing reduced to a  
655 minimum, concentration ratios between the MARGA and the reference denuder were

656 typically between 0.17 and 0.98 (10<sup>th</sup> and 90<sup>th</sup> percentile, G. Spindler and B. Stieger, personal  
657 communication). Using a value of 0.25 (lower quartile of the intercomparison) as a correction  
658 factor for nitric acid measured during HCCT-2010 (i.e. multiplying measured apparent  
659 concentrations by 4) yields upwind SEs for total nitrate between 0.7 and 1.2 (as event means),  
660 which would be more consistent with the values obtained for ammonium and sulfate.

661 An enrichment of cloud water nitrate has previously been observed in several studies and has  
662 usually been related to the uptake of nitric acid as the most probable explanation (Prabhakar  
663 et al., 2014; Hayden et al., 2008; Brüggemann et al., 2005; Sellegri et al., 2003; Cape et al.,  
664 1997), which is in agreement with our considerations described above.

665 In conclusion, the comparison of upwind and in-cloud scavenging efficiencies reveals that i)  
666 nucleation scavenging typically removed >80 %, often close to 100 % of soluble material  
667 from the particle phase upon cloud formation, ii) uptake of gaseous ammonia, nitric acid and  
668 water-soluble VOCs had an additional significant impact on observed cloud water  
669 concentrations, and iii) particulate material is clearly lost or diluted to some extent between  
670 the upwind and the in-cloud site, likely due to physical processes such as droplet scavenging  
671 by trees and/or entrainment of cleaner air masses.

672

### 673 **3.4 Size-resolved droplet compositions**

#### 674 **3.4.1 3-stage collector**

675 In Figure 7 volume-weighted mean (VWM) concentrations per cloud event are shown for  
676 ions, H<sub>2</sub>O<sub>2</sub>, and DOC within the droplet size classes of the 3-stage collector. Even though the  
677 nominal cut-off diameters of the 3 stages are given in Figure 7, it has to be noted, that in  
678 reality significant mixing of droplets between the nominal size classes occurs due to the  
679 relatively broad collection efficiency curves (Straub and Collett, 2002). Concentrations in a  
680 given droplet size class are thus influenced by droplets from other size classes to a significant  
681 extent and the size distributions can only reflect an approximate picture of the real pattern.

682 Volumes of cloud water collected per stage were between 5.9 and 240 ml with typically  
683 lowest volumes on the intermediate stage (16-22 µm) and highest volumes in the smaller or  
684 larger size class, depending on the sample (see Figure S8 for details).

685 Volume-weighted mean concentrations per event were calculated to reduce the complexity of  
686 the data set, even though information on the temporal evolution of size-resolved  
687 concentrations is lost by the averaging. Data for all individual samples taken with the 3-stage  
688 collector is given in the Supplemental Material (Figure S96 – Figure S158). As can be seen  
689 there, concentrations levels of individual cloud water constituents can vary significantly  
690 within one cloud event while the general patterns of concentrations in the three droplet size  
691 classes are often quite persistent during an event (exceptions will be noted below). For the  
692 major ions sulfate, nitrate, and ammonium, two main profiles of size-resolved cloud water  
693 concentrations can be observed in the VWM data: i) decreasing concentrations with  
694 increasing drop size for FCEs 1.1, 11.2, 11.3, 13.3, and ii) profiles with minimum  
695 concentrations in medium-sized droplets on stage 2 (“U”-shaped profiles) for FCEs 22.1 and  
696 FCE26.1+2. Only for nitrate during FCE1.1 a profile of increasing concentrations with  
697 increasing drop size is observed. Concentration differences between highest and lowest values  
698 are usually within a factor of 2 with the exception of FCE11.2, where concentrations of  
699 sulfate and ammonium in large drops were a factor of 3-4 lower than in small drops (on  
700 VWM basis). The two types of profiles reflect the dominant profiles of major ions in the  
701 individual samples (Figures S69 – Figure S811) for most of the events. Only during FCE1.1  
702 and mainly for sulfate and ammonium, the VWM profile does not adequately represent the  
703 individual profiles, which were rather variable during the first half of this 15h event and  
704 stabilized to a profile of increasing concentrations with increasing drop size during the second  
705 half of the event. As sampled water volumes were comparably low during the second half of  
706 the event, however, their weight to the volume-weighted mean profile is rather low. Literature  
707 data from 3-stage cloud water collectors is very sparse. Raja et al. (2008) report decreasing  
708 concentrations of main ions with increasing drop size for fog samples in the US Gulf coast  
709 region, obtained with the same collector as in the present study. Collett et al. (1995) observed  
710 U-type profiles in cloud samples obtained with a different 3-stage collector (different nominal  
711 cut-offs) from two sites in North Carolina and California, USA.

712 The VWM profiles of low concentration ions (chloride, sodium, magnesium, calcium, and –  
713 in part – potassium) were found to be markedly different from the major ion profiles.  
714 Concentrations were usually increasing with increasing drop size, especially for events with  
715 elevated concentrations (FCE1.1, 22.1, and 26.1+2) due to elevated impact of marine  
716 emissions on sampled air masses (cf. section 3.3.2). Also, observed concentration differences  
717 in different drop size ranges tended to be larger (up to a factor of 10) as compared to major

718 ion concentrations. Available literature data for minor ions in three drop size ranges reveals  
719 diverse profiles, depending on species and location (Raja et al., 2009; Collett et al., 1995).

720 In contrast to the ionic data, concentrations of H<sub>2</sub>O<sub>2</sub> in different collector stages were  
721 comparably homogeneous, with maximum differences of 25% (or a factor of 1.3). This is  
722 likely related to the different incorporation pathway (uptake from gas-phase as compared to  
723 nucleation scavenging for the ions), which is expected to yield more similar concentrations in  
724 differently sized cloud drops, at least if equilibrium conditions are assumed (Hoag et al.,  
725 1999).

726 Both uptake pathways can in principle occur for DOC (VOC uptake and/or dissolution of  
727 CCN organic material). The size-resolved concentration pattern in Figure 7, however,  
728 resembles those of major ions, suggesting nucleation scavenging as the major path of DOC  
729 incorporation into cloud water during this study.

730 Mean pH values per event (based on VWM concentrations of H<sup>+</sup>) are shown in Figure 8a. A  
731 similar pattern of slightly (approx. 0.1 pH units per stage) increasing values with increasing  
732 drop diameter can be observed for nearly all events and collector stages. In individual samples  
733 (Figure S169) differences between stages can be somewhat higher (up to approx. 0.5 pH  
734 units), but the general patterns look similar to the VWM event averages. Qualitatively,  
735 increasing pH with drop size is consistent with i) coarse (and typically less acidic) CCNs  
736 leading to larger droplets (cf. elevated concentrations of coarse particle mode constituents),  
737 and ii) reduced (diluted) concentrations of potentially acidic constituents (sulfate, nitrate,  
738 DOC) in larger drops (Collett et al., 1994).

739 These observations highlight the complexity of solute concentration drop size dependencies.  
740 Even for the comparably uniform conditions of the present study (same site, same season,  
741 similar air mass origins, similar heights within the cloud), different profiles can result for one  
742 and the same ion. This becomes even more obvious from individual samples (e.g. sulfate  
743 during FCE1.1, Figure S69), where – as stated above – a number of different profiles can  
744 occur during the same cloud event. Considering that these individual samples represent  
745 volume-weighted averages over 2 hours, it is easy to imagine that with a higher time  
746 resolution of sampling the variability of observed profiles would even increase. Without  
747 detailed numerical modelling (which is beyond the scope of this study), a quantitative  
748 understanding of these profiles and their variations seems impossible. In addition, the sampler  
749 characteristics (few stages with broad collection efficiencies) together with changing droplet

750 size distributions in a cloud might influence the observed size dependencies. Even though  
751 drop volume size distributions were usually similar both between events (Figure S1720) and  
752 between individual samples within the events (Figure S1821), subtle changes, e.g. in the  
753 broadness of the distribution or in the abundance of large ( $> 30 \mu\text{m}$ ) drops, can – together  
754 with the broad mixing of differently sized drops – lead to artificial modifications in the  
755 observed volume-weighted concentrations on the three stages (Moore et al., 2004a). Despite  
756 these difficulties, two broad conclusions from the 3-stage sf-CASCC ion data can be drawn:  
757 (i) main ions (sulfate, nitrate, ammonium) have similar solute concentration drop size  
758 dependencies (consistent with their presumed strong internal mixing in CCNs) and are often  
759 enriched in smaller sized droplets (even though other, especially U-type profiles do occur as  
760 well), and (ii) increasing concentrations with increasing droplet sizes, which might be  
761 expected based on the consideration of the simple Ogren et al. (1992) model (see section 1),  
762 are mainly observed if a strong coarse mode in upwind particles is present for a given  
763 constituent (e.g. for sodium, magnesium, chloride, and nitrate- during FCE1.1; cf. Figure  
764 S1922 and Figure S2023 for size distributions of inorganic ions at upwind site during FCEs).  
765 These findings are consistent with the availability of coarse CCN being an important  
766 prerequisite for such an inverse concentration – size relationship to develop (Schell et al.,  
767 1997), although other factors likely contribute to these observations as well.

768

### 769 3.4.2 5-stage collector

770 Size-resolved concentrations of ions and  $\text{H}_2\text{O}_2$  from the 5-stage collector are given in Figure 9  
771 in the same way as described above for the 3-stage data (event VWM and normalised data).  
772 Collected cloud water volumes were from 0.55 to 15 ml, with smallest volumes typically in  
773 the 4-10  $\mu\text{m}$  droplet size range and largest ones mostly for droplets  $>30 \mu\text{m}$  (see also Figure  
774 S24). eConcentration profiles of individual samples are shown in Figure S245 – Figure  
775 S2933). The number of events is smaller, as this sampler was not operated during FCE1.1 and  
776 FCE26.1+2. Due to the relatively low volume of cloud water the 5-stage collector is  
777 sampling, DOC analysis could not be performed from these samples. For major ions, the  
778 patterns are broadly consistent with the profiles of decreasing concentrations with increasing  
779 drop size observed from the 3-stage collector for FCEs 11.2, 11.3, and 13.3, with FCE22.1  
780 showing some similarity to a U-shape (even though the concentration increase towards larger  
781 drops is observable on stage 2 only, not on stage 1 collecting the largest drops). Concentration

782 differences between smallest and largest droplets are somewhat more pronounced (typically a  
783 factor of about 2) as compared to the 3-stage collector (typically smaller than a factor of 2),  
784 illustrating the higher efficiency of the 5-stage collector in separating small and large drop  
785 populations. Sharpest concentration differences are usually observed between stage 4 and 5  
786 (small droplets). This is true for basically all of the individual samples as well (Figure S254 –  
787 Figure S2933). Concentration patterns on stages 1-4, however, can vary somewhat within a  
788 single event, depending on the development of the cloud. For example, nitrate shows  
789 constantly decreasing concentrations with increasing drop sizes during the first half of  
790 FCE11.2 (Figure S226), while during the second half, concentrations in larger drops tend to  
791 increase. Similarly, ammonium concentrations develop from a maximum in medium-sized  
792 drops for the first sample to notably homogeneous concentrations across all 5 collector stages  
793 (difference of only about 30 % between smallest and largest drops) during FCE11.2 (Figure  
794 S237). The observed profiles differ from those reported from a hill cap cloud at Whiteface,  
795 NY, USA, using the same 5-stage collector (Moore et al., 2004a), where U-type profiles with  
796 highest concentrations in largest drops were observed for ammonium and nitrate, while  
797 sulfate showed increasing concentrations with increasing drop size through all 5 stages. The  
798 same study reports 5-stage concentration profiles from a fog event in Davis, CA, USA, which  
799 are more similar to those in this study, with decreasing concentrations with increasing drop  
800 size (Moore et al., 2004a).

801 The patterns of trace ions also show some similarity with the ones observed from the 3-stage  
802 collector, mainly in that concentrations tend to increase from medium-sized towards larger  
803 droplets for most ions and events as well. There are, however, two distinct features in the 5-  
804 stage data which are not captured by the 3-stage collector: First, similar to the main ions, the  
805 concentration increase towards larger droplets is often (though not always) observable on  
806 stage 2 only, with decreasing concentrations on stage 1 (largest drops). Second, all trace ions  
807 show a very pronounced concentration increase in smallest droplets (stage 5), with often a  
808 factor of 5-10 difference to stage 4 concentrations, which is usually not seen in the 3-stage  
809 data, where smallest droplets are mixed with much larger ones on stage 3, leading to more  
810 diluted concentrations. Literature data on size-resolved trace ion concentrations from 5-stage  
811 collectors is available only for calcium, for which a pronounced U-type profile with highest  
812 concentrations in largest drops was reported (Moore et al., 2004a), while sodium, potassium  
813 and chloride ions were mentioned to have very similar profiles.



814 Compared to ionic content, the concentrations of H<sub>2</sub>O<sub>2</sub> are more homogeneously distributed  
815 between the collector stages (maximum deviation < 50%) - similar to what was observed from  
816 the 3-stage collector data - and a general pattern cannot be observed from the (few) data  
817 available.

818 Event-averaged pH values from the 5-stage collector are given in Figure 8b (for individual  
819 samples in Figure S304). Highest values were mostly observed in smallest droplets (stage 5)  
820 with a significant decrease towards the next droplet size range (stage 4) at least during 3 out  
821 of the 4 events. From collector stage 4 towards stage 2 (increasing drop sizes) pH values tend  
822 to increase, similar to what is observed from the 3-stage collector (Figure 8a), while in largest  
823 drops (stage 1) they decrease again (to different extents). -Overall, pH variations between  
824 different drop size classes are not too large for the sampled clouds with maximum differences  
825 of about 0.6 pH units on event-averaged basis.

826 These observations are generally consistent with the findings from the 3-stage collector.  
827 However, they also highlight the higher efficiency of drop population separation of the 5-  
828 stage collector as compared to the 3-stage collector, as ratios between minimum and  
829 maximum concentrations are larger and the sharp concentration increase towards the smallest  
830 droplets (especially for trace ions) is only observed here (for volume size droplet distributions  
831 during 5-stage sampling see Figure S345). In addition, the observation of often decreasing  
832 concentrations from stage 2 (second-largest drops) to stage 1 (largest drops) might reflect the  
833 transition from region II (condensation growth) to region III (coalescence growth) in the  
834 Ogren et al. (1992) model (section 1), even though it must be noted that collection efficiency  
835 curves of these two stages are overlapping to a comparatively large extent (Straub and Collett,  
836 2002). Compared to the study of Moore et al. (2004a) stressing the importance of cloud age  
837 (drop growth time) by comparing two different types of clouds/fogs, our data from more  
838 similar cloud systems highlights the impact of the size distributions of CCN constituents on  
839 the development of size-resolved concentration patterns. Both parameters were predicted to  
840 be relevant from detailed model sensitivity studies (section 1, Schell et al., 1997). In addition,  
841 despite the considerable mixing of droplets with different sizes occurring in the samplers, the  
842 data reveal the substantial differences which can exist in different droplet size classes as well  
843 as the variability of observed solute concentration profiles even under comparably similar  
844 cloud conditions. As such differences impact both chemical reactions in cloud drops and  
845 deposition efficiencies and can thus modify atmospheric sink and/or source strengths of PM

846 constituents (Moore et al., 2004b), further observational and modelling studies on size-  
847 resolved droplet compositions seem important.

848

#### 849 **4 Conclusions**

850 The analysis of bulk and size-resolved cloud water samples and related measurements of 8  
851 cloud events during HCCT-2010 has led to the following main conclusions:

- 852 | - Variability of solute concentrations in bulk samples was high ~~even~~ for the ~~comparably~~  
853 | ~~uniform conditions~~ clouds studied during the campaign and was caused mainly by the  
854 | variability of CCN concentrations and compositions, i.e. air mass history, in contrast  
855 | to earlier suggestion of LWC generally being the main driver in solute concentration  
856 | variation.
- 857 | - A simple functional relationship between LWC and solute concentrations was  
858 | observed only within single cloud events with little variation in incoming air mass  
859 | concentrations and conditions. Across several events, no single factor is available to  
860 | adequately describe the complex processes determining observed solute  
861 | concentrations in cloud water. If a simple function is needed,  $R_{\text{eff}}$  might be a  
862 | somewhat better choice than LWC.
- 863 | - Both nucleation scavenging and gas-phase uptake contributed to observed cloud water  
864 | concentrations of major constituents, with the first one being especially important for  
865 | sulfate and the second one for nitrate.
- 866 | - Losses of particulate mass occur from the upwind to the in-cloud site, observed from  
867 | different in-cloud vs. upwind scavenging efficiencies and likely related to physical  
868 | loss processes such as droplet scavenging and/or entrainment.
- 869 | - Solute concentration droplet size profiles can be highly variable even within single  
870 | events and were only partly consistent with considerations from a simple conceptual  
871 | model. The observations made highlight the importance of CCN constituents' size  
872 | distributions on the development of concentration profiles, consistent with earlier  
873 | numerical simulation results.
- 874 | - The comprehensive dataset obtained during HCCT-2010 will serve as a reference for  
875 | the further development and evaluation of multiphase models in future studies.

876

877 Supplemental material related to this article is available online at doi: ...

878

## 879 **Acknowledgements**

880 The authors acknowledge the support of several TROPOS staff members during cloud water  
881 sampling (even at unearthly hours), Jenoptik for providing the Ceilometer, the German  
882 Federal Environmental Agency (UBA) for providing the MARGA (contract 35101070) and  
883 the German Weather Service (DWD) and UBA for their cooperation and support at the  
884 Schmücke field site. HCCT-2010 was partially funded by the German Research Foundation  
885 (DFG) under contract HE 3086/15-1. The participation of Stephan Mertes was funded by the  
886 DFG priority program HALO (SPP 1294, grant HE 939/25-1). Partial additional support for  
887 Colorado State University was provided by the U.S. National Science Foundation (AGS-  
888 0711102 and AGS-1050052).

889

## 890 **References**

- 891 Acker, K., Möller, D., Marquardt, W., Brüggemann, E., Wieprecht, W., Auel, R., and Kalass,  
892 D.: Atmospheric research program for studying changing emission patterns after  
893 German unification, *Atmospheric Environment*, 32, 3435-3443, doi: 10.1016/S1352-  
894 2310(98)00041-7, 1998.
- 895 Acker, K., Mertes, S., Moller, D., Wieprecht, W., Auel, R., and Kalass, D.: Case study of  
896 cloud physical and chemical processes in low clouds at Mt. Brocken, *Atmospheric*  
897 *Research*, 64, 41-51, doi: 10.1016/S0169-8095(02)00078-9, 2002.
- 898 Aleksic, N., and Dukett, J. E.: Probabilistic relationship between liquid water content and ion  
899 concentrations in cloud water, *Atmospheric Research*, 98, 400-405, doi:  
900 10.1016/j.atmosres.2010.08.003, 2010.
- 901 Bator, A., and Collett, J. L.: Cloud chemistry varies with drop size, *J. Geophys. Res.-Atmos.*,  
902 102, 28071-28078, doi: 10.1029/97jd02306, 1997.
- 903 Benedict, K. B., Lee, T., and Collett, J. L.: Cloud water composition over the southeastern  
904 Pacific Ocean during the VOCALS regional experiment, *Atmospheric Environment*,  
905 46, 104-114, doi: 10.1016/j.atmosenv.2011.10.029, 2012.
- 906 Beswick, K. M., Choulaton, T. W., Inglis, D. W. F., Dore, A. J., and Fowler, D.: Influences  
907 on long-term trends in ion concentration and deposition at Holme Moss, *Atmospheric*  
908 *Environment*, 37, 1927-1940, doi: 10.1016/S1352-2310(03)00046-3, 2003.
- 909 Blas, M., Sobik, M., and Twarowski, R.: Changes of cloud water chemical composition in the  
910 Western Sudety Mountains, Poland, *Atmospheric Research*, 87, 224-231, doi:  
911 10.1016/j.atmosres.2007.11.004, 2008.

- 912 Brantner, B., Fierlinger, H., Puxbaum, H., and Berner, A.: Cloudwater Chemistry in the  
913 Subcooled Droplet Regime at Mount-Sonnblick (3106-M Asl, Salzburg, Austria),  
914 *Water Air Soil Poll*, 74, 363-384, 1994.
- 915 Bridges, K. S., Jickells, T. D., Davies, T. D., Zeman, Z., and Hunova, I.: Aerosol,  
916 precipitation and cloud water chemistry observations on the Czech Krusne Hory  
917 plateau adjacent to a heavily industrialised valley, *Atmospheric Environment*, 36, 353-  
918 360, doi: 10.1016/S1352-2310(01)00388-0, 2002.
- 919 Brüggemann, E., Gnauk, T., Mertes, S., Acker, K., Auel, R., Wieprecht, W., Möller, D.,  
920 Collett, J. L., Chang, H., Galgon, D., Chemnitzer, R., Rüd, C., Junek, R.,  
921 Wiedensohler, W., and Herrmann, H.: Schmücke hill cap cloud and valley stations  
922 aerosol characterisation during FEBUKO (I): Particle size distribution, mass, and main  
923 components, *Atmospheric Environment*, 39, 4291-4303, doi:  
924 10.1016/j.atmosenv.2005.02.013, 2005.
- 925 Cape, J. N., Hargreaves, K. J., StoretonWest, R. L., Jones, B., Davies, T., Colvile, R. N.,  
926 Gallagher, M. W., Choularton, T. W., Pahl, S., Berner, A., Kruisz, C., Bizjak, M., Laj,  
927 P., Facchini, M. C., Fuzzi, S., Arends, B. G., Acker, K., Wieprecht, W., Harrison, R.  
928 M., and Peak, J. D.: The budget of oxidised nitrogen species in orographic clouds,  
929 *Atmospheric Environment*, 31, 2625-2636, doi: 10.1016/S1352-2310(96)00192-6,  
930 1997.
- 931 Collett, J. L., Daube, B., Munger, J. W., and Hoffmann, M. R.: Cloud water chemistry in  
932 Sequoia National Park, *Atmospheric Environment*, 23, 999-1007, 1989.
- 933 Collett, J. L., Bator, A., Rao, X., and Demoz, B. B.: Acidity Variations across the Cloud Drop  
934 Size Spectrum and Their Influence on Rates of Atmospheric Sulfate Production,  
935 *Geophysical Research Letters*, 21, 2393-2396, doi: Doi 10.1029/94gl02480, 1994.
- 936 Collett, J. L., Iovinelli, R., and Demoz, B.: A three-stage cloud impactor for size-resolved  
937 measurement of cloud drop chemistry, *Atmospheric Environment*, 29, 1145-1154, doi:  
938 10.1016/1352-2310(94)00338-1, 1995.
- 939 Collett, J. L., Sherman, D. E., Moore, K. F., Hannigan, M. P., and Lee, T.: Aerosol particle  
940 processing and removal by fogs: Observations in chemically heterogeneous central  
941 California radiation fogs, *Water, Air, and Soil Pollution: Focus*, 1, 303-312, 2001.
- 942 Collett, J. L., Herckes, P., Youngster, S., and Lee, T.: Processing of atmospheric organic  
943 matter by California radiation fogs, *Atmospheric Research*, 87, 232-241, doi:  
944 10.1016/j.atmosres.2007.11.005, 2008.
- 945 Dasgupta, P. K., Decesare, K., and Ullrey, J. C.: Determination of Atmospheric Sulfur-  
946 Dioxide without Tetrachloromercurate(Ii) and the Mechanism of the Schiff Reaction,  
947 *Analytical Chemistry*, 52, 1912-1922, doi: 10.1021/Ac50062a031, 1980.
- 948 Daum, P. H., Kelly, T. J., Schwartz, S. E., and Newman, L.: Measurements of the Chemical  
949 Composition of Stratiform Clouds, *Atmospheric Environment*, 18, 2671-2684, doi:  
950 10.1016/0004-6981(84)90332-9, 1984.
- 951 Deguillaume, L., Charbouillot, T., Joly, M., Vaïtilingom, M., Parazols, M., Marinoni, A.,  
952 Amato, P., Delort, A. M., Vinatier, V., Flossmann, A., Chaumerliac, N., Pichon, J. M.,  
953 Houdier, S., Laj, P., Sellegri, K., Colomb, A., Brigante, M., and Mailhot, G.:  
954 Classification of clouds sampled at the puy de Dôme (France) based on 10 yr of

- 955 monitoring of their physicochemical properties, *Atmospheric Chemistry and Physics*,  
956 14, 1485-1506, doi: 10.5194/acp-14-1485-2014, 2014.
- 957 Demoz, B. B., Collett, J. L., and Daube, B. C.: On the Caltech Active Strand Cloudwater  
958 Collectors, *Atmospheric Research*, 41, 47-62, doi: 10.1016/0169-8095(95)00044-5,  
959 1996.
- 960 Draxler, R. R., and Rolph, G. D.: HYSPLIT (HYbrid Single-Particle Lagrangian Integrated  
961 Trajectory) Model access via NOAA ARL READY Website  
962 (<http://www.arl.noaa.gov/ready/hysplit4.html>). NOAA Air Resources Laboratory,  
963 Silver Spring, MD, 2003.
- 964 EEA: European Union emission inventory report 1990–2012 under the UNECE Convention  
965 on Long-range Transboundary Air Pollution (LRTAP), European Environment  
966 Agency (EEA), Luxembourg, Technical Report 12/2014, 130 pp., doi: 10.2800/18374,  
967 2014.
- 968 Elbert, W., Hoffmann, M. R., Kramer, M., Schmitt, G., and Andreae, M. O.: Control of solute  
969 concentrations in cloud and fog water by liquid water content, *Atmospheric  
970 Environment*, 34, 1109-1122, doi: 10.1016/S1352-2310(99)00351-9, 2000.
- 971 Elbert, W., Kramer, M., and Andreae, M. O.: Reply to discussion on "Control of solute  
972 concentrations in cloud and fog water by liquid water content", *Atmospheric  
973 Environment*, 36, 1909-1910, doi: Pii S1352-2310(02)00143-7  
974 10.1016/S1352-2310(02)00143-7, 2002.
- 975 Facchini, M. C., Mircea, M., Fuzzi, S., and Charlson, R. J.: Cloud albedo enhancement by  
976 surface-active organic solutes in growing droplets, *Nature*, 401, 257-259, doi:  
977 10.1038/45758, 1999.
- 978 Fahey, K. M., Pandis, S. N., Collett, J. L., and Herckes, P.: The influence of size-dependent  
979 droplet composition on pollutant processing by fogs, *Atmospheric Environment*, 39,  
980 4561-4574, doi: 10.1016/j.atmosenv.2005.04.006, 2005.
- 981 Flossmann, A. I., and Wobrock, W.: A review of our understanding of the aerosol–cloud  
982 interaction from the perspective of a bin resolved cloud scale modelling, *Atmospheric  
983 Research*, 97, 478-497, doi: 10.1016/j.atmosres.2010.05.008, 2010.
- 984 Fowler, D., Pilegaard, K., Sutton, M. A., Ambus, P., Raivonen, M., Duyzer, J., Simpson, D.,  
985 Fagerli, H., Fuzzi, S., Schjoerring, J. K., Granier, C., Neftel, A., Isaksen, I. S. A., Laj,  
986 P., Maione, M., Monks, P. S., Burkhardt, J., Daemmgen, U., Neiryneck, J., Personne,  
987 E., Wichink-Kruit, R., Butterbach-Bahl, K., Flechard, C., Tuovinen, J. P., Coyle, M.,  
988 Gerosa, G., Loubet, B., Altimir, N., Gruenhage, L., Ammann, C., Cieslik, S., Paoletti,  
989 E., Mikkelsen, T. N., Ro-Poulsen, H., Cellier, P., Cape, J. N., Horvath, L., Loreto, F.,  
990 Niinemets, U., Palmer, P. I., Rinne, J., Misztal, P., Nemitz, E., Nilsson, D., Pryor, S.,  
991 Gallagher, M. W., Vesala, T., Skiba, U., Brüeggemann, N., Zechmeister-Boltenstern,  
992 S., Williams, J., O'Dowd, C., Facchini, M. C., de Leeuw, G., Flossman, A.,  
993 Chaumerliac, N., and Erisman, J. W.: Atmospheric composition change: Ecosystems-  
994 Atmosphere interactions, *Atmospheric Environment*, 43, 5193-5267, doi:  
995 10.1016/j.atmosenv.2009.07.068, 2009.
- 996 Gilardoni, S., Massoli, P., Giulianelli, L., Rinaldi, M., Paglione, M., Pollini, F., Lanconelli,  
997 C., Poluzzi, V., Carbone, S., Hillamo, R., Russell, L. M., Facchini, M. C., and Fuzzi,

- 998 S.: Fog scavenging of organic and inorganic aerosol in the Po Valley, *Atmospheric*  
999 *Chemistry and Physics*, 14, 6967-6981, doi: 10.5194/acp-14-6967-2014, 2014.
- 1000 Giulianelli, L., Gilardoni, S., Tarozzi, L., Rinaldi, M., Decesari, S., Carbone, C., Facchini, M.  
1001 C., and Fuzzi, S.: Fog occurrence and chemical composition in the Po valley over the  
1002 last twenty years, *Atmospheric Environment*, 98, 394-401, doi:  
1003 10.1016/j.atmosenv.2014.08.080, 2014.
- 1004 Gurciullo, C. S., and Pandis, S. N.: Effect of composition variations in cloud droplet  
1005 populations on aqueous-phase chemistry, *J. Geophys. Res.-Atmos.*, 102, 9375-9385,  
1006 doi: 10.1029/96jd03651, 1997.
- 1007 Harris, E., Sinha, B., van Pinxteren, D., Tilgner, A., Fomba, K. W., Schneider, J., Roth, A.,  
1008 Gnauk, T., Fahlbusch, B., Mertes, S., Lee, T., Collett, J., Foley, S., Borrmann, S.,  
1009 Hoppe, P., and Herrmann, H.: Enhanced Role of Transition Metal Ion Catalysis  
1010 During In-Cloud Oxidation of SO<sub>2</sub>, *Science*, 340, 727-730, doi:  
1011 10.1126/science.1230911, 2013.
- 1012 Harris, E., Sinha, B., van Pinxteren, D., Schneider, J., Poulain, L., Collett, J., D'Anna, B.,  
1013 Fahlbusch, B., Foley, S., Fomba, K. W., George, C., Gnauk, T., Henning, S., Lee, T.,  
1014 Mertes, S., Roth, A., Stratmann, F., Borrmann, S., Hoppe, P., and Herrmann, H.: In-  
1015 cloud sulfate addition to single particles resolved with sulfur isotope analysis during  
1016 HCCT-2010, *Atmospheric Chemistry and Physics*, 14, 4219-4235, doi: 10.5194/acp-  
1017 14-4219-2014, 2014.
- 1018 Hayden, K. L., Macdonald, A. M., Gong, W., Toom-Sauntry, D., Anlauf, K. G., Leithead, A.,  
1019 Li, S. M., Leaitch, W. R., and Noone, K.: Cloud processing of nitrate, *J. Geophys.*  
1020 *Res.-Atmos.*, 113, -, doi: 10.1029/2007jd009732, 2008.
- 1021 Hegg, D. A., Hobbs, P. V., and Radke, L. F.: Measurements of the Scavenging of Sulfate and  
1022 Nitrate in Clouds, *Atmospheric Environment*, 18, 1939-1946, doi: 10.1016/0004-  
1023 6981(84)90371-8, 1984.
- 1024 Hegg, D. A., Gao, S., and Jonsson, H.: Measurements of selected dicarboxylic acids in marine  
1025 cloud water, *Atmospheric Research*, 62, 1-10, doi: 10.1016/S0169-8095(02)00023-6,  
1026 2002.
- 1027 Herckes, P., Wendling, R., Sauret, N., Mirabel, P., and Wortham, H.: Cloudwater studies at a  
1028 high elevation site in the Vosges Mountains (France), *Environ Pollut*, 117, 169-177,  
1029 doi: 10.1016/S0269-7491(01)00139-7, 2002.
- 1030 Herckes, P., Valsaraj, K. T., and Collett, J. L.: A review of observations of organic matter in  
1031 fogs and clouds: Origin, processing and fate, *Atmospheric Research*, 132-133, 434-  
1032 449, doi: 10.1016/j.atmosres.2013.06.005, 2013.
- 1033 Herrmann, H., Wolke, R., Müller, K., Brüggemann, E., Gnauk, T., Barzagli, P., Mertes, S.,  
1034 Lehmann, K., Massling, A., Birmili, W., Wiedensohler, A., Wieprecht, W., Acker, K.,  
1035 Jaeschke, W., Kramberger, H., Svrčina, B., Bächmann, K., Collett, J. L., Galgon, D.,  
1036 Schwirn, K., Nowak, A., van Pinxteren, D., Plewka, A., Chemnitzer, R., Rüd, C.,  
1037 Hofmann, D., Tilgner, A., Diehl, K., Heinold, B., Hinneburg, D., Knoth, O., Sehili, A.  
1038 M., Simmel, M., Wurzler, S., Majdik, Z., Mauersberger, G., and Müller, F.: FEBUKO  
1039 and MODMEP: Field measurements and modelling of aerosol and cloud multiphase  
1040 processes, *Atmospheric Environment*, 39, 4169-4183, 2005.

- 1041 Herrmann, H., Schaefer, T., Tilgner, A., Styler, S. A., Weller, C., Teich, M., and Otto, T.:  
1042 Tropospheric Aqueous-Phase Chemistry: Kinetics, Mechanisms, and Its Coupling to a  
1043 Changing Gas Phase, *Chemical Reviews*, 150507133427007, doi: 10.1021/cr500447k,  
1044 2015.
- 1045 Hitzenberger, R., Berner, A., Kromp, R., Kasper-Giebl, A., Limbeck, A., Tschewenka, W.,  
1046 and Puxbaum, H.: Black carbon and other species at a high-elevation European site  
1047 (Mount Sonnblick, 3106 m, Austria): Concentrations and scavenging efficiencies, *J.*  
1048 *Geophys. Res.-Atmos.*, 105, 24637-24645, doi: 10.1029/2000jd900349, 2000.
- 1049 Hoag, K. J., Collett, J. L., and Pandis, S. N.: The influence of drop size-dependent fog  
1050 chemistry on aerosol processing by San Joaquin Valley fogs, *Atmospheric*  
1051 *Environment*, 33, 4817-4832, doi: 10.1016/S1352-2310(99)00268-X, 1999.
- 1052 Joos, F., and Baltensperger, U.: A Field-Study on Chemistry, S(IV) Oxidation Rates and  
1053 Vertical Transport during Fog Conditions, *Atmos Environ a-Gen*, 25, 217-230, doi:  
1054 10.1016/0960-1686(91)90292-F, 1991.
- 1055 Kasper-Giebl, A., Koch, A., Hitzenberger, R., and Puxbaum, H.: Scavenging efficiency of  
1056 'aerosol carbon' and sulfate in supercooled clouds at Mt. Sonnblick (3106 m a.s.l.,  
1057 Austria), *J Atmos Chem*, 35, 33-46, doi: 10.1023/A:1006250508562, 2000.
- 1058 Kasper-Giebl, A.: Control of solute concentrations in cloud and fog water by liquid water  
1059 content, *Atmospheric Environment*, 36, 1907-1908, doi: 10.1016/S1352-  
1060 2310(02)00147-4, 2002.
- 1061 Khwaja, H. A.: Atmospheric concentrations of carboxylic acids and related compounds at a  
1062 semiurban site, *Atmospheric Environment*, 29, 127-139, doi: 10.1016/1352-  
1063 2310(94)00211-3, 1995.
- 1064 Laj, P., Fuzzi, S., Facchini, M. C., Lind, J. A., Orsi, G., Preiss, M., Maser, R., Jaeschke, W.,  
1065 Seyffer, E., Helas, G., Acker, K., Wieprecht, W., Moller, D., Arends, B. G., Mols, J.  
1066 J., Colvile, R. N., Gallagher, M. W., Beswick, K. M., Hargreaves, K. J., StoretonWest,  
1067 R. L., and Sutton, M. A.: Cloud processing of soluble gases, *Atmospheric*  
1068 *Environment*, 31, 2589-2598, doi: 10.1016/S1352-2310(97)00040-X, 1997.
- 1069 Lammel, G., and Metzger, G.: Multiphase Chemistry of Orographic Clouds - Observations at  
1070 Sub-Alpine Mountain Sites, *Fresen J Anal Chem*, 340, 564-574, doi:  
1071 10.1007/Bf00322431, 1991.
- 1072 Lazrus, A. L., Kok, G. L., Gitlin, S. N., Lind, J. A., and McLaren, S. E.: Automated  
1073 fluorimetric method for hydrogen peroxide in atmospheric precipitation, *Analytical*  
1074 *Chemistry*, 57, 917-922, doi: 10.1021/ac00281a031, 1985.
- 1075 Leitch, W. R., Strapp, J. W., Wiebe, H. A., Anlauf, K. G., and Isaac, G. A.: Chemical and  
1076 Microphysical Studies of Nonprecipitating Summer Cloud in Ontario, Canada, *J.*  
1077 *Geophys. Res.-Atmos.*, 91, 1821-1831, doi: 10.1029/Jd091id11p11821, 1986.
- 1078 Löflund, M., Kasper-Giebl, A., Schuster, B., Giebl, H., Hitzenberger, R., and Puxbaum, H.:  
1079 Formic, acetic, oxalic, malonic and succinic acid concentrations and their contribution  
1080 to organic carbon in cloud water, *Atmospheric Environment*, 36, 1553-1558, 2002.
- 1081 Marinoni, A., Laj, P., Sellegri, K., and Mailhot, G.: Cloud chemistry at the Puy de Dome:  
1082 variability and relationships with environmental factors, *Atmospheric Chemistry and*  
1083 *Physics*, 4, 715-728, 2004.

- 1084 Marinoni, A., Parazols, M., Brigante, M., Deguillaume, L., Amato, P., Delort, A.-M., Laj, P.,  
1085 and Mailhot, G.: Hydrogen peroxide in natural cloud water: Sources and  
1086 photoreactivity, *Atmospheric Research*, 101, 256-263, doi:  
1087 10.1016/j.atmosres.2011.02.013, 2011.
- 1088 Mertes, S., Galgon, D., Schwirn, K., Nowak, A., Lehmann, K., Massling, A., Wiedensohler,  
1089 A., and Wieprecht, W.: Evolution of particle concentration and size distribution  
1090 observed upwind, inside and downwind hill cap clouds at connected flow conditions  
1091 during FEBUKO, *Atmospheric Environment*, 39, 4233-4245, doi:  
1092 10.1016/j.atmosenv.2005.02.009, 2005.
- 1093 Möller, D., Acker, K., and Wieprecht, W.: A relationship between liquid water content and  
1094 chemical composition in clouds, *Atmospheric Research*, 41, 321-335, doi:  
1095 10.1016/0169-8095(96)00017-8, 1996.
- 1096 Moore, K. F., Sherman, D. E., Reilly, J. E., and Collett, J. L.: Development of a multi-stage  
1097 cloud water collector Part 1: Design and field performance evaluation, *Atmospheric*  
1098 *Environment*, 36, 31-44, doi: 10.1016/S1352-2310(01)00476-9, 2002.
- 1099 Moore, K. F., Sherman, D. E., Reilly, J. E., and Collett, J. L.: Drop size-dependent chemical  
1100 composition in clouds and fogs. Part I. Observations, *Atmospheric Environment*, 38,  
1101 1389-1402, doi: 10.1016/j.atmosenv.2003.12.013, 2004a.
- 1102 Moore, K. F., Sherman, D. E., Reilly, J. E., Hannigan, M. P., Lee, T., and Collett, J. L.: Drop  
1103 size-dependent chemical composition of clouds and fogs. Part II: Relevance to  
1104 interpreting the aerosol/trace gas/fog system, *Atmospheric Environment*, 38, 1403-  
1105 1415, doi: 10.1016/j.atmosenv.2003.12.014, 2004b.
- 1106 Neuman, J. A., Huey, L. G., Ryerson, T. B., and Fahey, D. W.: Study of Inlet Materials for  
1107 Sampling Atmospheric Nitric Acid, *Environmental science & technology*, 33, 1133-  
1108 1136, doi: 10.1021/es980767f, 1999.
- 1109 Noone, K. J., Ogren, J. A., Hallberg, A., Heintzenberg, J., Strom, J., Hansson, H.-C.,  
1110 Svenningsson, B., Wiedensohler, A., Fuzzi, S., Facchini, M. C., Arends, B. G., and  
1111 Berner, A.: Changes in aerosol size- and phase distributions due to physical and  
1112 chemical processes in fog, *Tellus B*, 44, 489-504, doi: 10.1034/j.1600-0889.1992.t01-  
1113 4-00004.x, 1992.
- 1114 Ogren, J. A., and Charlson, R. J.: Implications for models and measurements of chemical  
1115 inhomogeneities among cloud droplets, *Tellus B*, 44, 208-225, doi: 10.1034/j.1600-  
1116 0889.1992.t01-2-00004.x, 1992.
- 1117 Ogren, J. A., Noone, K. J., Hallberg, A., Heintzenberg, J., Schell, D., Berner, A., Solly, I.,  
1118 Kruisz, C., Reischl, G., Arends, B. G., and Wobrock, W.: Measurements of the size  
1119 dependence of the concentration of nonvolatile material in fog droplets, *Tellus B*, 44,  
1120 570-580, doi: 10.1034/j.1600-0889.1992.t01-1-00010.x, 1992.
- 1121 Phillips, G. J., Makkonen, U., Schuster, G., Sobanski, N., Hakola, H., and Crowley, J. N.: The  
1122 detection of nocturnal N<sub>2</sub>O<sub>5</sub> as HNO<sub>3</sub> by alkali- and aqueous-denuder techniques,  
1123 *Atmospheric Measurement Techniques*, 6, 231-237, doi: 10.5194/amt-6-231-2013,  
1124 2013.
- 1125 Prabhakar, G., Ervens, B., Wang, Z., Maudlin, L. C., Coggon, M. M., Jonsson, H. H.,  
1126 Seinfeld, J. H., and Sorooshian, A.: Sources of nitrate in stratocumulus cloud water:



- 1127 Airborne measurements during the 2011 E-PEACE and 2013 NiCE studies,  
1128 Atmospheric Environment, 97, 166-173, doi: 10.1016/j.atmosenv.2014.08.019, 2014.
- 1129 Pruppacher, H. R., and Klett, J. D.: Concentrations of water soluble compounds in individual  
1130 cloud and raindrops, chapter 17.3 in: Microphysics of clouds and precipitation, 2nd  
1131 ed., Springer, New York, 954 pp., 2010.
- 1132 R Core Team: R: A language and environment for statistical computing: [http://www.R-](http://www.R-project.org)  
1133 [project.org](http://www.R-project.org), 2015.
- 1134 Raja, S., Raghunathan, R., Yu, X. Y., Lee, T. Y., Chen, J., Kommalapati, R. R., Murugesan,  
1135 K., Shen, X., Qingzhong, Y., Valsaraj, K. T., and Collett, J. L.: Fog chemistry in the  
1136 Texas-Louisiana Gulf Coast corridor, Atmospheric Environment, 42, 2048-2061, doi:  
1137 10.1016/j.atmosenv.2007.12.004, 2008.
- 1138 Raja, S., Raghunathan, R., Kommalapati, R. R., Shen, X. H., Collett, J. L., and Valsaraj, K.  
1139 T.: Organic composition of fogwater in the Texas-Louisiana gulf coast corridor,  
1140 Atmospheric Environment, 43, 4214-4222, doi: 10.1016/j.atmosenv.2009.05.029,  
1141 2009.
- 1142 Rao, X., and Collett, J. L.: Behavior of S(IV) and Formaldehyde in a Chemically  
1143 Heterogeneous Cloud, Environmental science & technology, 29, 1023-1031, doi:  
1144 10.1021/es00004a024, 1995.
- 1145 Reilly, J. E., Rattigan, O. V., Moore, K. F., Judd, C., Sherman, D. E., Dutkiewicz, V. A.,  
1146 Kreidenweis, S. M., Husain, L., and Collett, J. L.: Drop size-dependent S(IV)  
1147 oxidation in chemically heterogeneous radiation fogs, Atmospheric Environment, 35,  
1148 5717-5728, doi: 10.1016/S1352-2310(01)00373-9, 2001.
- 1149 Roth, A., Schneider, J., Klimach, T., Mertes, S., van Pinxteren, D., Herrmann, H., and  
1150 Borrmann, S.: Aerosol properties, source identification, and cloud processing in  
1151 orographic clouds measured by single particle mass spectrometry on a Central  
1152 European mountain site during HCCT-2010, Atmospheric Chemistry and Physics,  
1153 accepted 19 December 2015, doi: 10.5194/acp-16-1-2016, 2016.
- 1154 Rumsey, I. C., Cowen, K. A., Walker, J. T., Kelly, T. J., Hanft, E. A., Mishoe, K., Rogers, C.,  
1155 Proost, R., Beachley, G. M., Lear, G., Frelink, T., and Otjes, R. P.: An assessment of  
1156 the performance of the Monitor for AeRosols and GAses in ambient air (MARGA): a  
1157 semi-continuous method for soluble compounds, Atmospheric Chemistry and Physics,  
1158 14, 5639-5658, doi: 10.5194/acp-14-5639-2014, 2014.
- 1159 Schell, D., Wobrock, W., Maser, R., Preiss, M., Jaeschke, W., Georgii, H. W., Gallagher, M.  
1160 W., Bower, K. N., Beswick, K. M., Pahl, S., Facchini, M. C., Fuzzi, S., Wiedensohler,  
1161 A., Hansson, H. C., and Wendisch, M.: The size-dependent chemical composition of  
1162 cloud droplets, Atmospheric Environment, 31, 2561-2576, doi: 10.1016/S1352-  
1163 2310(96)00286-5, 1997.
- 1164 Schwarzenböck, A., Heintzenberg, J., and Mertes, S.: Incorporation of aerosol particles  
1165 between 25 and 850 nm into cloud elements: measurements with a new  
1166 complementary sampling system, Atmospheric Research, 52, 241-260, 2000.
- 1167 Seinfeld, J. H., and Pandis, S. N.: Atmospheric chemistry and physics : From air pollution to  
1168 climate change -2nd edition, 2nd ed., Wiley, New York, 1326 pp., 2006.
- 1169 Sellegri, K.: Size-dependent scavenging efficiencies of multicomponent atmospheric aerosols  
1170 in clouds, Journal of Geophysical Research, 108, doi: 10.1029/2002jd002749, 2003.

- 1171 Sellegri, K., Laj, P., Marinoni, A., Dupuy, R., Legrand, M., and Preunkert, S.: Contribution of  
 1172 gaseous and particulate species to droplet solute composition at the Puy de Dome,  
 1173 France, *Atmospheric Chemistry and Physics*, 3, 1509-1522, 2003.
- 1174 Spiess, A.-N., and Neumeyer, N.: An evaluation of R2 as an inadequate measure for nonlinear  
 1175 models in pharmacological and biochemical research: a Monte Carlo approach, *BMC*  
 1176 *pharmacology*, 10, doi: 10.1186/1471-2210-10-6, 2010.
- 1177 Straub, D. J., and Collett, J. L.: Development of a multi-stage cloud water collector Part 2:  
 1178 Numerical and experimental calibration, *Atmospheric Environment*, 36, 45-56, doi:  
 1179 10.1016/S1352-2310(01)00477-0, 2002.
- 1180 Straub, D. J., Hutchings, J. W., and Herckes, P.: Measurements of fog composition at a rural  
 1181 site, *Atmospheric Environment*, 47, 195-205, doi: 10.1016/j.atmosenv.2011.11.014,  
 1182 2012.
- 1183 Svenningsson, B., Hansson, H. C., Martinsson, B., Wiedensohler, A., Swietlicki, E.,  
 1184 Cederfelt, S. I., Wendisch, M., Bower, K. N., Choulaton, T. W., and Colvile, R. N.:  
 1185 Cloud droplet nucleation scavenging in relation to the size and hygroscopic behaviour  
 1186 of aerosol particles, *Atmospheric Environment*, 31, 2463-2475, doi: 10.1016/S1352-  
 1187 2310(96)00179-3, 1997.
- 1188 Taraniuk, I., Kostinski, A. B., and Rudich, Y.: Enrichment of surface-active compounds in  
 1189 coalescing cloud drops, *Geophysical Research Letters*, 35, -, doi:  
 1190 10.1029/2008gl034973, 2008.
- 1191 Tilgner, A., Schöne, L., Bräuer, P., van Pinxteren, D., Hoffmann, E., Spindler, G., Styler, S.  
 1192 A., Mertes, S., Birmili, W., Otto, R., Merkel, M., Weinhold, K., Wiedensohler, A.,  
 1193 Deneke, H., Schrödner, R., Wolke, R., Schneider, J., Haunold, W., Engel, A., Wéber,  
 1194 A., and Herrmann, H.: Comprehensive assessment of meteorological conditions and  
 1195 airflow connectivity during HCCT-2010, *Atmospheric Chemistry and Physics*, 14,  
 1196 9105-9128, doi: 10.5194/acp-14-9105-2014, 2014.
- 1197 van Pinxteren, D., Plewka, A., Hofmann, D., Müller, K., Kramberger, H., Svrčina, B.,  
 1198 Bächmann, K., Jaeschke, W., Mertes, S., Collett, J. L., and Herrmann, H.: Schmücke  
 1199 hill cap cloud and valley stations aerosol characterisation during FEBUKO (II):  
 1200 Organic compounds, *Atmospheric Environment*, 39, 4305-4320, doi:  
 1201 10.1016/j.atmosenv.2005.02.014, 2005.
- 1202 van Pinxteren, D., Brüggemann, E., Gnauk, T., Inuma, Y., Müller, K., Nowak, A., Achtert,  
 1203 P., Wiedensohler, A., and Herrmann, H.: Size- and time-resolved chemical particle  
 1204 characterization during CAREBeijing-2006: Different pollution regimes and diurnal  
 1205 profiles, *J. Geophys. Res.-Atmos.*, 114, doi: 10.1029/2008jd010890, 2009.
- 1206 van Pinxteren, D., Brüggemann, E., Gnauk, T., Müller, K., Thiel, C., and Herrmann, H.: A  
 1207 GIS based approach to back trajectory analysis for the source apportionment of  
 1208 aerosol constituents and its first application, *J Atmos Chem*, 67, 1-28, doi:  
 1209 10.1007/s10874-011-9199-9, 2010.
- 1210 Vet, R., Artz, R. S., Carou, S., Shaw, M., Ro, C.-U., Aas, W., Baker, A., Bowersox, V. C.,  
 1211 Dentener, F., Galy-Lacaux, C., Hou, A., Pienaar, J. J., Gillett, R., Forti, M. C.,  
 1212 Gromov, S., Hara, H., Khodzher, T., Mahowald, N. M., Nickovic, S., Rao, P. S. P.,  
 1213 and Reid, N. W.: A global assessment of precipitation chemistry and deposition of  
 1214 sulfur, nitrogen, sea salt, base cations, organic acids, acidity and pH, and phosphorus,  
 1215 *Atmospheric Environment*, 93, 3-100, doi: 10.1016/j.atmosenv.2013.10.060, 2014.

1216 Whalley, L. K., Stone, D., George, I. J., Mertes, S., van Pinxteren, D., Tilgner, A., Herrmann,  
1217 H., Evans, M. J., and Heard, D. E.: The influence of clouds on radical concentrations:  
1218 observations and modelling studies of HO<sub>x</sub> during the Hill Cap Cloud Thuringia  
1219 (HCCT) campaign in 2010, *Atmospheric Chemistry and Physics*, 15, 3289-3301, doi:  
1220 10.5194/acp-15-3289-2015, 2015.

1221 Wickham, H.: *ggplot2: Elegant graphics for data analysis*, Springer, New York, 2009.

1222 Wrzesinsky, T., and Klemm, O.: Summertime fog chemistry at a mountainous site in central  
1223 Europe, *Atmospheric Environment*, 34, 1487-1496, doi: 10.1016/S1352-  
1224 2310(99)00348-9, 2000.

1225 Zimmermann, L., and Zimmermann, F.: Fog deposition to Norway Spruce stands at high-  
1226 elevation sites in the Eastern Erzgebirge (Germany), *J Hydrol*, 256, 166-175, doi:  
1227 10.1016/S0022-1694(01)00532-7, 2002.

1228

1229

1230

1231

1232 **Tables and Figures**

1233

1234

**Table 1: Sampling times of cloud water collectors during Full Cloud Events with mean liquid water content (LWC), droplet surface area (PSA), effective droplet radius ( $R_{\text{eff}}$ ), Schmücke above cloud base (SACB), temperature (T), wind speed (WS), and global radiation (GR) at Mt. Schmücke, as well as the number of samples for the different collectors.**

Event	Start (CEST)	Stop (CEST)	Duration (h)	LWC ( $\text{g m}^{-3}$ )	SACB (m)	PSA ( $\text{cm}^2 \text{m}^{-3}$ )	$R_{\text{eff}}$ ( $\mu\text{m}$ )	T ( $^{\circ}\text{C}$ )	WS ( $\text{m s}^{-1}$ )	GR ( $\text{W m}^{-2}$ )	# CASCC2	# 3-stage	# 5-stage
FCE1.1	14/09/2010 11:00	15/09/2010 02:00	15	0.24	167	1248	5.7	9.2	8.2	15	15	7	- <sup>a</sup>
FCE7.1	24/09/2010 23:45	25/09/2010 01:45	2	0.19	156	846	5.7	8.3	5.5	0	2	1	1
FCE11.2	01/10/2010 22:30	02/10/2010 05:30	7	0.37	237	1277	8.7	6.2	4.1	0	7	4	4
FCE11.3	02/10/2010 14:30	02/10/2010 19:30	5	0.33	225	1353	7.4	7.7	7.3	31	5	3	2
FCE13.3	06/10/2010 12:15	07/10/2010 03:15	15	0.34	185	1392	7.3	9.1	3.9	52	15	8	4
FCE22.1	19/10/2010 21:30	20/10/2010 03:30	6	0.30	222	1272	7.4	1.2	4.7	0	6	3	2
FCE26.1	24/10/2010 01:30	24/10/2010 08:30	7	0.20	174	961	7.6	2.3	8.9	0	7	3	- <sup>a</sup>
FCE26.2	24/10/2010 09:15	24/10/2010 11:45	2.5	0.14	141	701	7.3	1.4	9.1	43	3	1	- <sup>a</sup>

a) Collector not operated

1 **Table 2: Summary of cloud water solute concentrations determined during HCCT-2010.**

Compound	Unit	#	Range	median	mean	VWM
pH		60	3.6-5.3	4.56	4.29 <sup>a</sup>	4.30 <sup>a</sup>
SO <sub>4</sub> <sup>2-</sup>	μmol L <sup>-1</sup>	60	6.2-104	33	43	39
NO <sub>3</sub> <sup>-</sup>	μmol L <sup>-1</sup>	60	46-479	151	164	142
Cl <sup>-</sup>	μmol L <sup>-1</sup>	60	3.7-84	22	30	25
NH <sub>4</sub> <sup>+</sup>	μmol L <sup>-1</sup>	60	64-523	182	216	191
Na <sup>+</sup>	μmol L <sup>-1</sup>	60	0.58-195	20	35	27
K <sup>+</sup>	μmol L <sup>-1</sup>	60	1.3-31	3.8	6.1	5.5
Mg <sup>2+</sup>	μmol L <sup>-1</sup>	60	0.63-26	3.1	5.1	4.1
Ca <sup>2+</sup>	μmol L <sup>-1</sup>	60	1.4-37	7	9.8	8.7
H <sub>2</sub> O <sub>2</sub>	μmol L <sup>-1</sup>	60	0.35-17	5	5.6	5.4
S(IV)	μmol L <sup>-1</sup>	34	BDL-3.6	2.1	1.9	1.9
HMS	μmol L <sup>-1</sup>	34	BDL-2.7	0.76	0.87	0.91
DOC	mgC L <sup>-1</sup>	60	1.3-13	4	4.4	3.9

2 #: Number of samples analysed

3 VWM: volume-weighted mean concentration

4 BDL: below detection limit

5 <sup>a</sup> derived from mean/VWM H<sup>+</sup> concentration

**Table 3: Comparison of mean HCCT-2010 cloud water concentrations with literature data (arithmetic or volume-weighted means) from other European mountain sites.**

Location	Date	pH	Cl <sup>-</sup> (μM)	SO <sub>4</sub> <sup>2-</sup> (μM)	NO <sub>3</sub> <sup>-</sup> (μM)	NH <sub>4</sub> <sup>+</sup> (μM)	Na <sup>+</sup> (μM)	K <sup>+</sup> (μM)	Mg <sup>2+</sup> (μM)	Ca <sup>2+</sup> (μM)	H <sub>2</sub> O <sub>2</sub> (μM)	DOC (mg L <sup>-1</sup> )	S(IV) (μM)	Ref.
Schmücke, Germany	2010	4.3	30	43	164	216	35	6.1	5.1	9.8	5.6	4.4	1.9	This work
Puy de Dome, France <sup>a</sup>	2001-2011	4.3	69	60	417	233	44	18	3.8	53	4.9	12 <sup>d</sup>		(Deguillaume et al., 2014)
Puy de Dome, France <sup>b</sup>	2001-2011	5.1	35	49	111	145	34	5.0	6.6	15	10	5.5 <sup>d</sup>		(Deguillaume et al., 2014)
Sudety Mts., Poland	2003-2004	4.25	66	67	173	167	67	6	10	26				(Blas et al., 2008)
Schmücke, Germany	2001-2002	4.5	19	59	207						2.7	6.4		(Brüggemann et al., 2005)
Holme Moss, UK <sup>c</sup>	1994-2001		652-1711	90-208 <sup>e</sup>	175-469	158-518	578-1563							(Beswick et al., 2003)
Rax, Austria	1999-2000	3.8	16	82	136	230	16	7	11	11		6.0 <sup>d</sup>		(Löflund et al., 2002)
Vosges Mts., France	1998-1999	4.82	143	149	181	276	175	57	26	60				(Herckes et al., 2002)
Zinnwald, Germany	1997-1998	4.0	48	281	176	560	52	23	6	28				(Zimmermann and Zimmermann, 2002)
Waldstein, Germany	1997	4.3	54	248	481	669	65	11.5	19.5	34				(Wrzesinsky and Klemm, 2000)
Krusne Hory, Czech Rep.	1995-1996	2.96	155	625	726	203	64	20	20	68				(Bridges et al., 2002)
Brocken, Germany <sup>c</sup>	1992-1996	3.8-4.5	68-119	133-160	280-365	378-468	60-128	2-12	14-18	27-67				(Acker et al., 1998)
Great Dun Fell, UK	1993	4.0		91	202	321							2.7	(Laj et al., 1997)
Sonnblick, Austria	1991 <sup>f</sup>	4.5	30	64	32	36	34	12	2.9	11				(Brantner et al., 1994)
Vosges Mts., France	1990	3.3	120	185	410	270	170	40					24	(Lammel and Metzsig, 1991)
Schöllkopf, Germany	1988	4.1	90	250	400	830	70	60						(Lammel and Metzsig, 1991)
Zindelen, Switzerland	1986-1987	4.8	431	447	1020	2107							85.9	(Joos and Baltensperger, 1991)

- a) polluted regime
- b) continental regime
- c) range of annual means
- d) TOC
- e) nss-Sulfate
- f) fall data

**Table 4: Factor loadings of 4 principal components after Varimax rotation. Loadings with absolute values  $\leq 0.2$  are regarded insignificant and omitted, while those  $> 0.6$  are regarded highly significant and printed bold.**

	F1	F2	F3	F4
pH		0.53	-0.26	-0.36
LWC	-0.57	-0.32		0.47
Reff	-0.45	<b>-0.74</b>		
RTI Water	<b>0.84</b>		-0.48	
RTI NaturalVegetation	<b>-0.92</b>		0.28	
RTI Agriculture	-0.39		<b>0.63</b>	0.49
RTI Urban	0.22			<b>0.91</b>
Sulfate		<b>0.93</b>		
Nitrate		<b>0.73</b>	0.54	0.24
Ammonium		<b>0.97</b>		
Sodium	<b>0.95</b>			
Magnesium	<b>0.89</b>		0.24	0.20
Chloride	<b>0.95</b>			
Potassium			<b>0.87</b>	
Calcium	0.26	0.34	<b>0.72</b>	0.34
DOC	-0.24	<b>0.77</b>	0.50	

**Table 5: Event means of upwind and in-cloud scavenging efficiencies calculated from different approaches. Numbers in brackets include both particulate and gaseous upwind concentrations, where available. See text for details.**

<b>Event</b>	<b>CASCC2+MARGA</b>	<b>CASCC2+INT-AMS</b>	<b>CVI/INT AMS</b>
<b>Ammonium</b>			
FCE1.1	0.85 (0.39)	0.92	0.83
FCE11.2	0.95 (0.52)	0.98	0.96
FCE11.3	1.04 (0.5)	0.97	0.97
FCE13.3	0.94 (0.65)	0.80	0.71
FCE22.1	0.85 (0.69)	0.96	0.96
FCE26.1+2	1.01 (0.51)	0.95	0.90
<b>Nitrate</b>			
FCE1.1	0.87 (0.82)	0.95	0.86
FCE11.2	2.26 (1.86)	0.99	0.95
FCE11.3	1.16 (1.01)	0.96	0.96
FCE13.3	1.17 (1.1)	0.87	0.79
FCE22.1	1.25 (1.18)	0.98	0.96
FCE26.1+2	1.04 (0.94)	0.96	0.94
<b>Sulfate</b>			
FCE1.1	0.66	0.88	0.79
FCE11.2	0.55	0.79	0.69
FCE11.3	0.79	0.89	0.88
FCE13.3	0.89	0.68	0.56
FCE22.1	0.82	0.94	0.94
FCE26.1+2	0.75	0.94	0.91
<b>DOC</b>			
FCE1.1	1.09a	0.83	0.67
FCE11.2	3.42a	0.86	0.88
FCE11.3	1.86a	0.89	0.92
FCE13.3	1.11a	0.72	0.69
FCE22.1	1.72a	0.87	0.79
FCE26.1+2	1.45a	0.89	0.86

a) DOC from MARGA not available. PM<sub>10</sub> water-soluble organic carbon from Berner impactor used instead.



## Figures

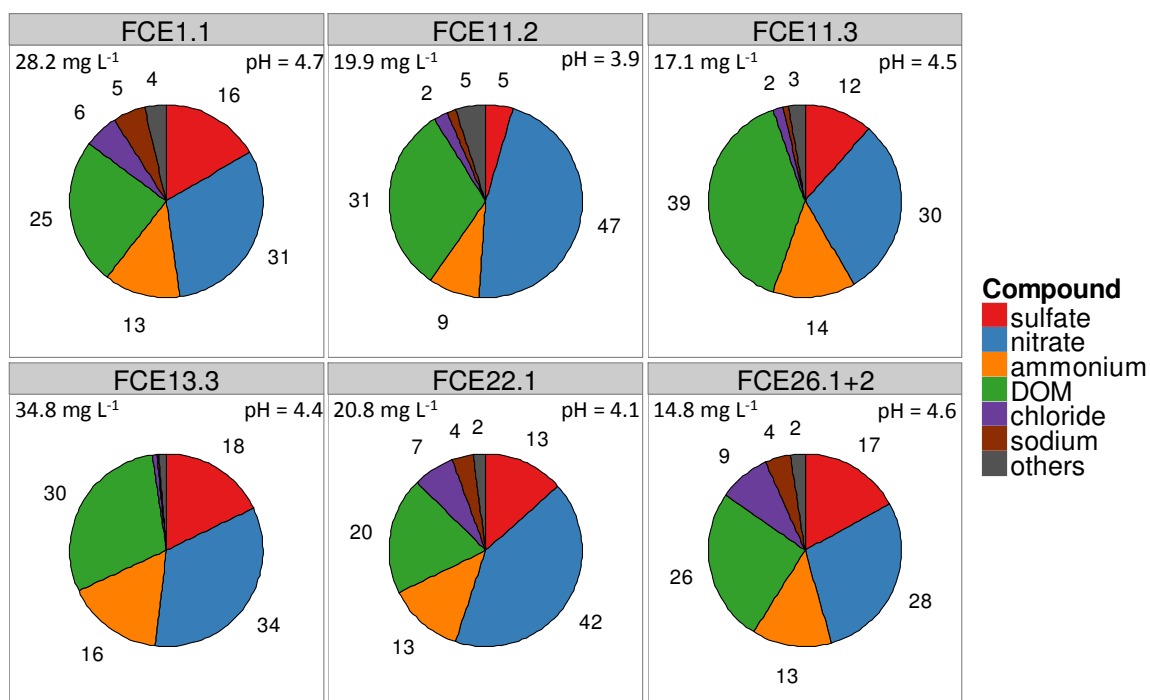


**Figure 1: Volume-weighted mean composition of bulk cloud water during main events. Numbers represent percentage from total solute concentration (in mg L<sup>-1</sup>). Trace solutes calcium, magnesium, potassium, H<sub>2</sub>O<sub>2</sub>(aq), and S(IV) are summarised as „others“. DOM is calculated as DOC\*1.8. Total solute concentrations and pH values derived from VWM H<sup>+</sup> concentrations are indicated in the upper left and reight panel corners, respectively.**

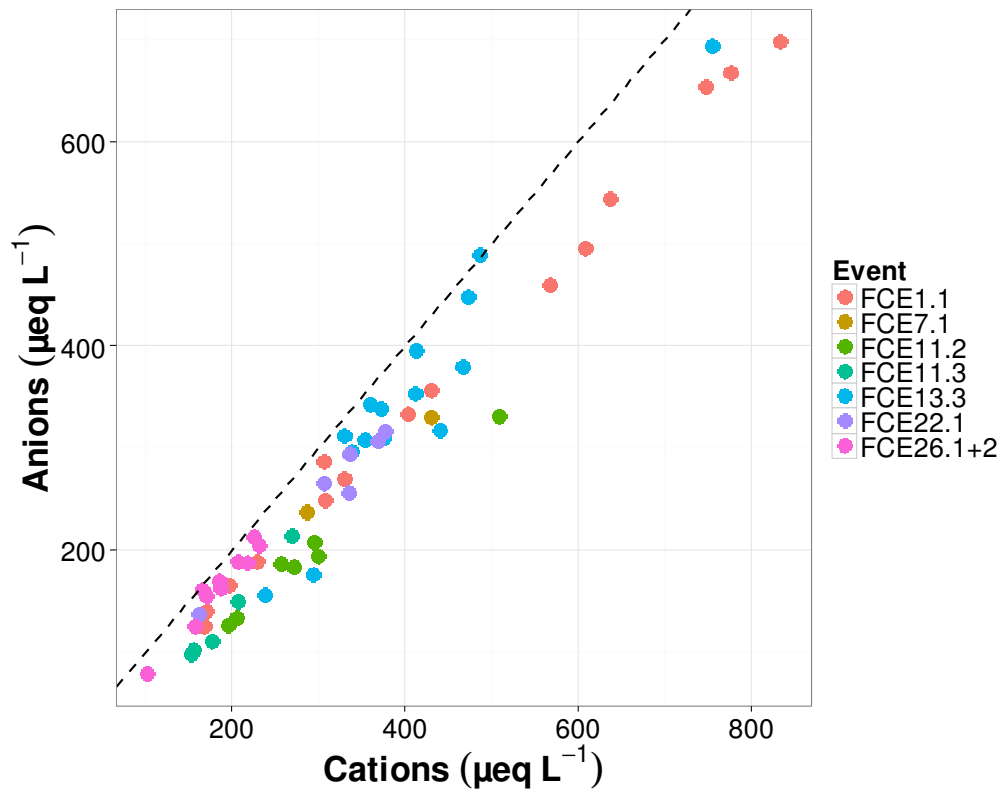


Figure 2: Ion balance on an equivalent basis for inorganic anions and cations. Dashed line is 1:1.

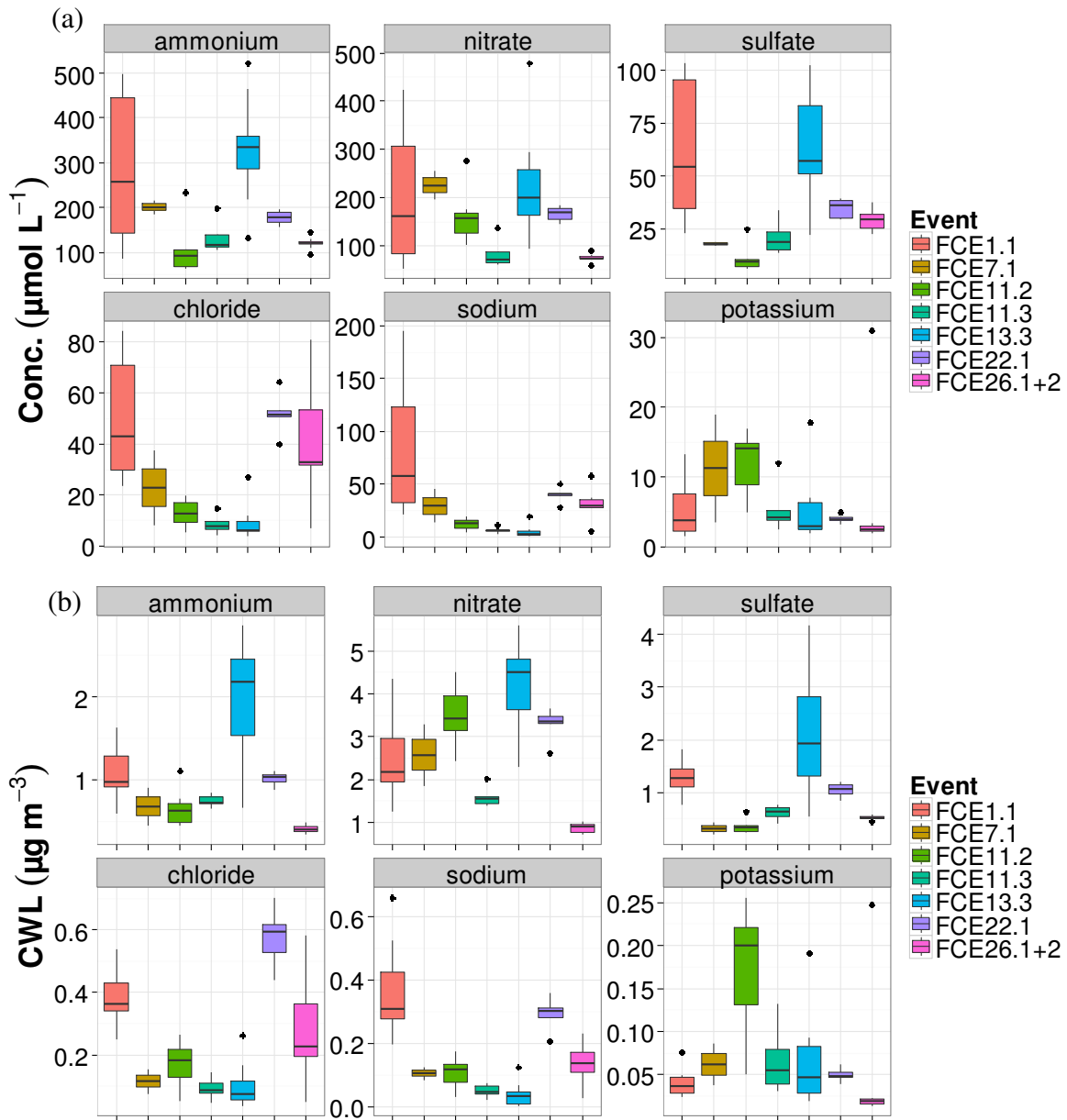
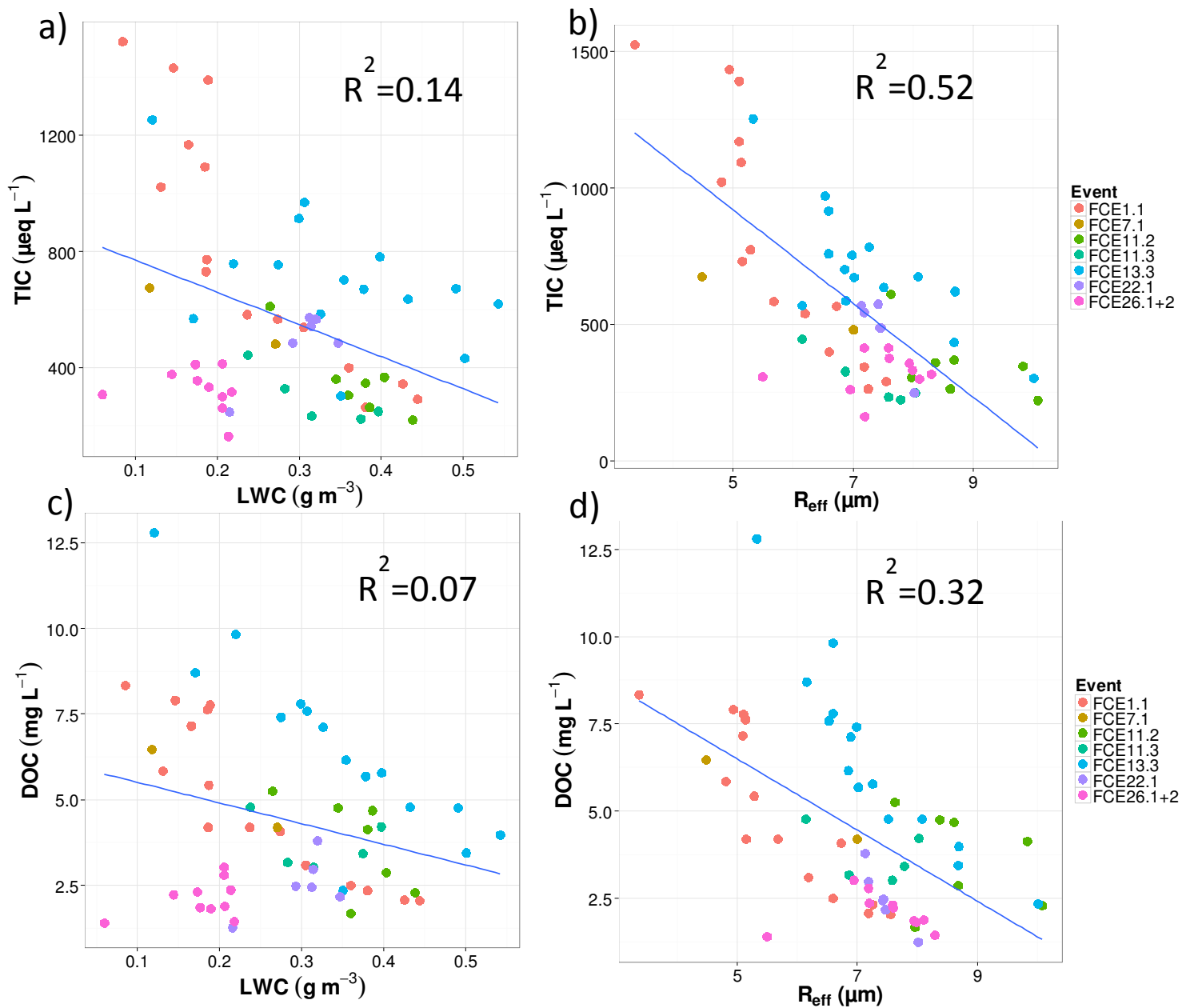
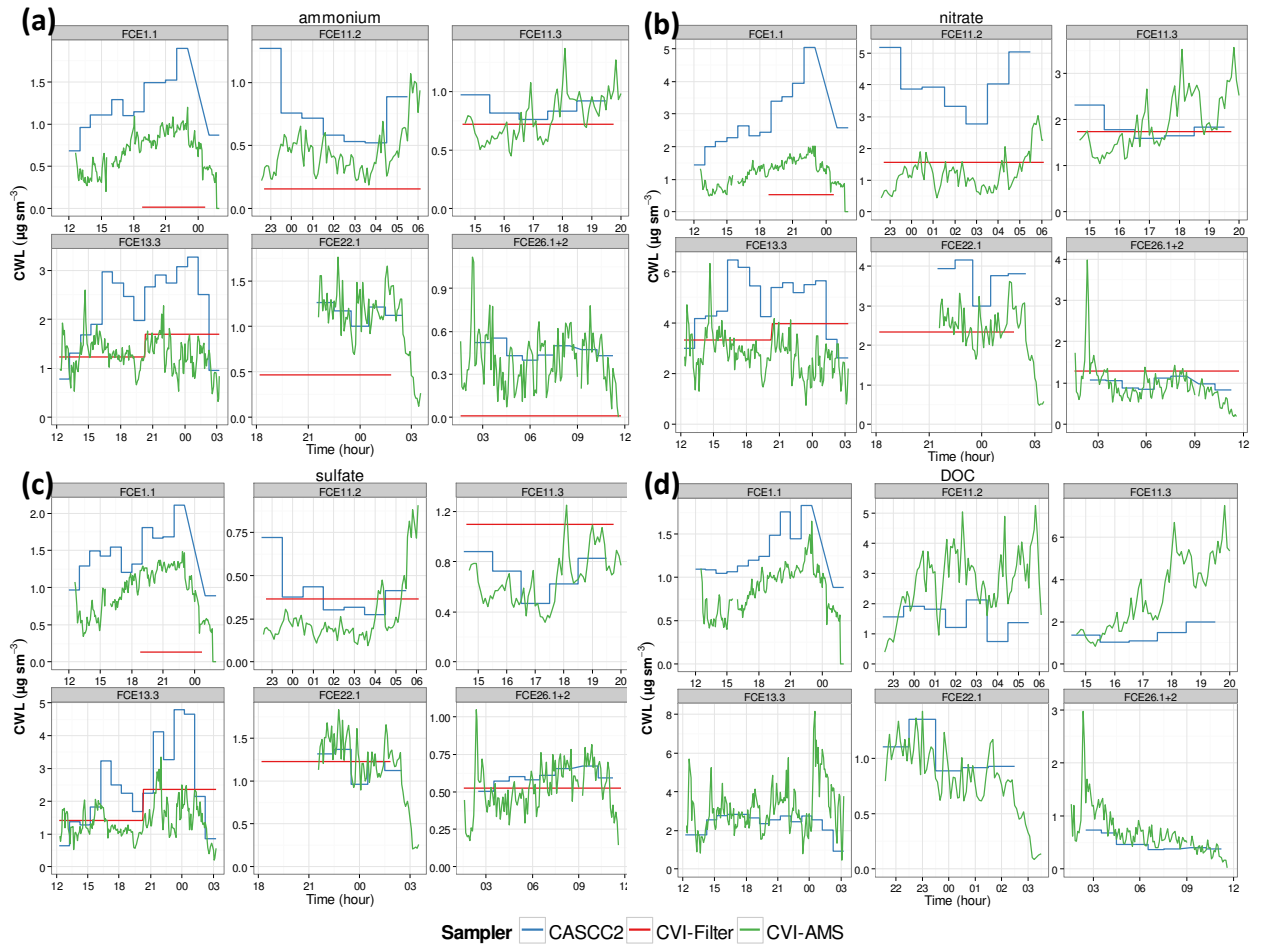


Figure 3: Variability of cloud water concentrations both within and between FCEs for selected inorganic ions. (a) Solute concentrations, (b) Cloud water loadings. Boxes indicate 25th, 50th, and 75th percentile, while whiskers extend to 1.5 \* IQR (interquartile range), and dots indicate individual data points outside this range.



**Figure 4: Relationships of total ionic content (upper panels) and dissolved organic carbon (lower panels) versus liquid water content (a and c) and effective droplet radius (b and d) for bulk cloud water samples.**



**Figure 5: Comparison of cloud water loadings (normalised to standard temperature and pressure) from bulk cloud water collector (blue), quartz filter downstream CVI inlet (red), and AMS downstream CVI (green) for cloud water main constituents (a) ammonium, (b) nitrate, (c) sulfate, and (d) DOC (AMS organics/1.8).**

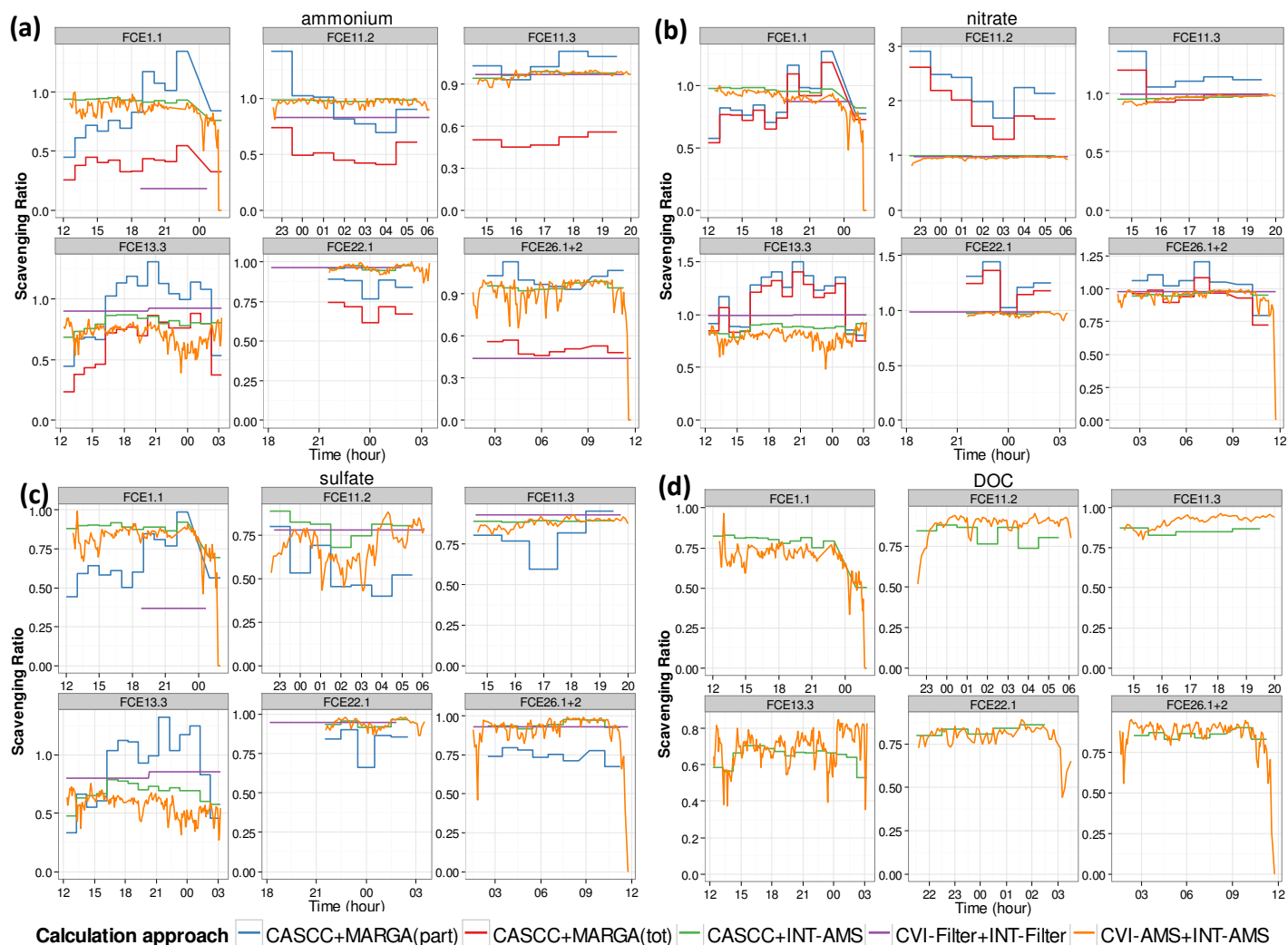


**Figure 6: Cloud scavenging efficiencies for (a) ammonium, (b) nitrate, (c) sulfate, and (d) DOC, calculated as “upwind SE” from bulk cloud water loadings and upwind MARGA data (blue and red for MARGA particulate and total aerosol concentrations, respectively) and “in-cloud SEs” from bulk CWLs and interstitial AMS data (green), droplet residual and interstitial particle concentrations from filters (purple), and droplet residual and interstitial particle concentrations from AMS (orange). See text for details.**

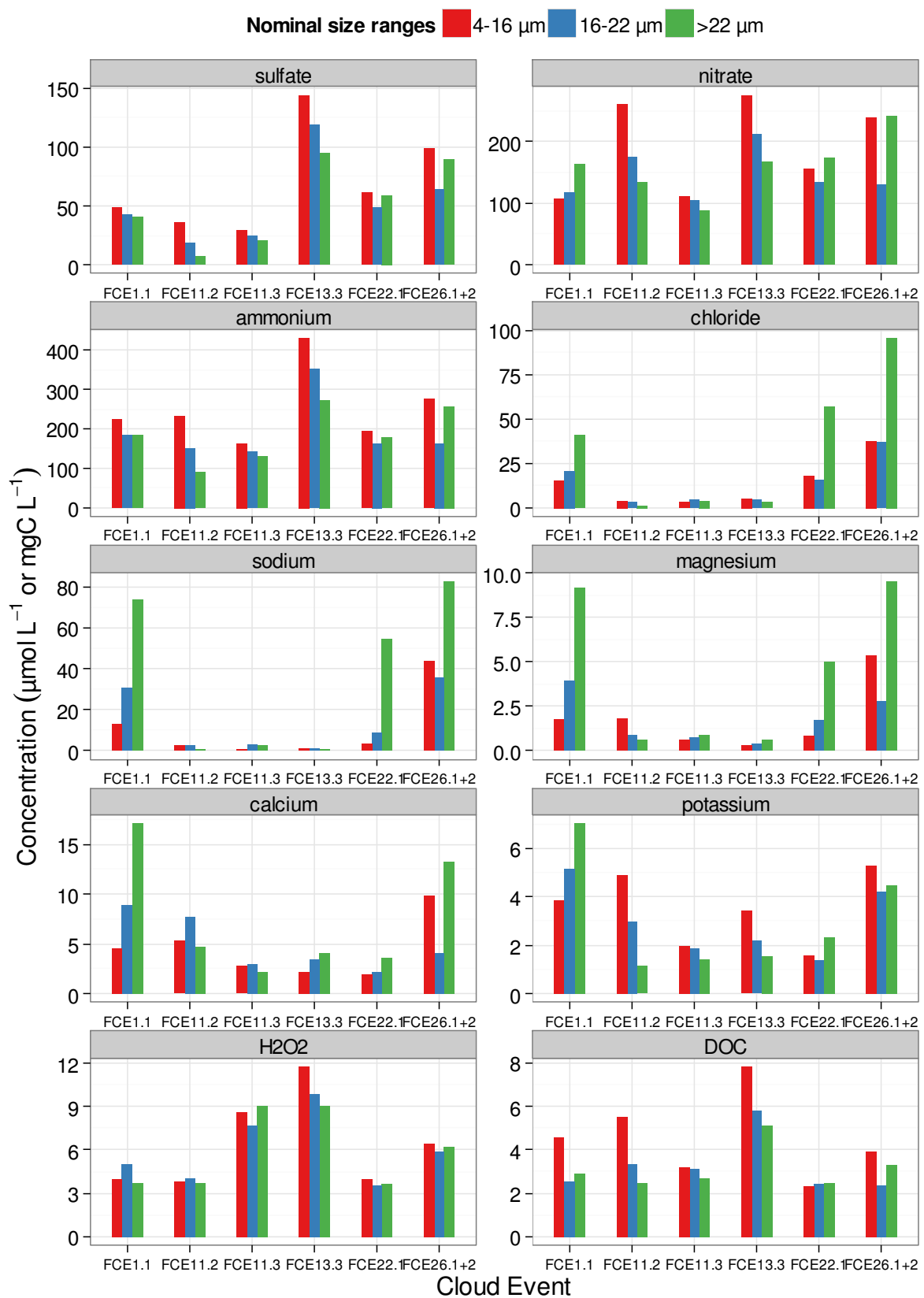
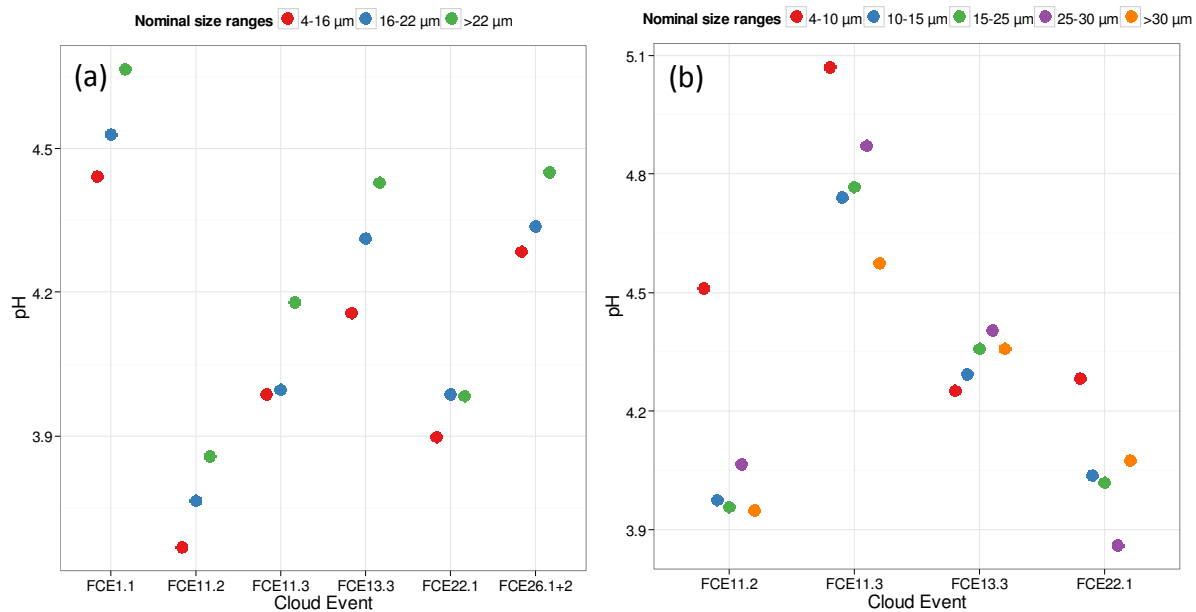
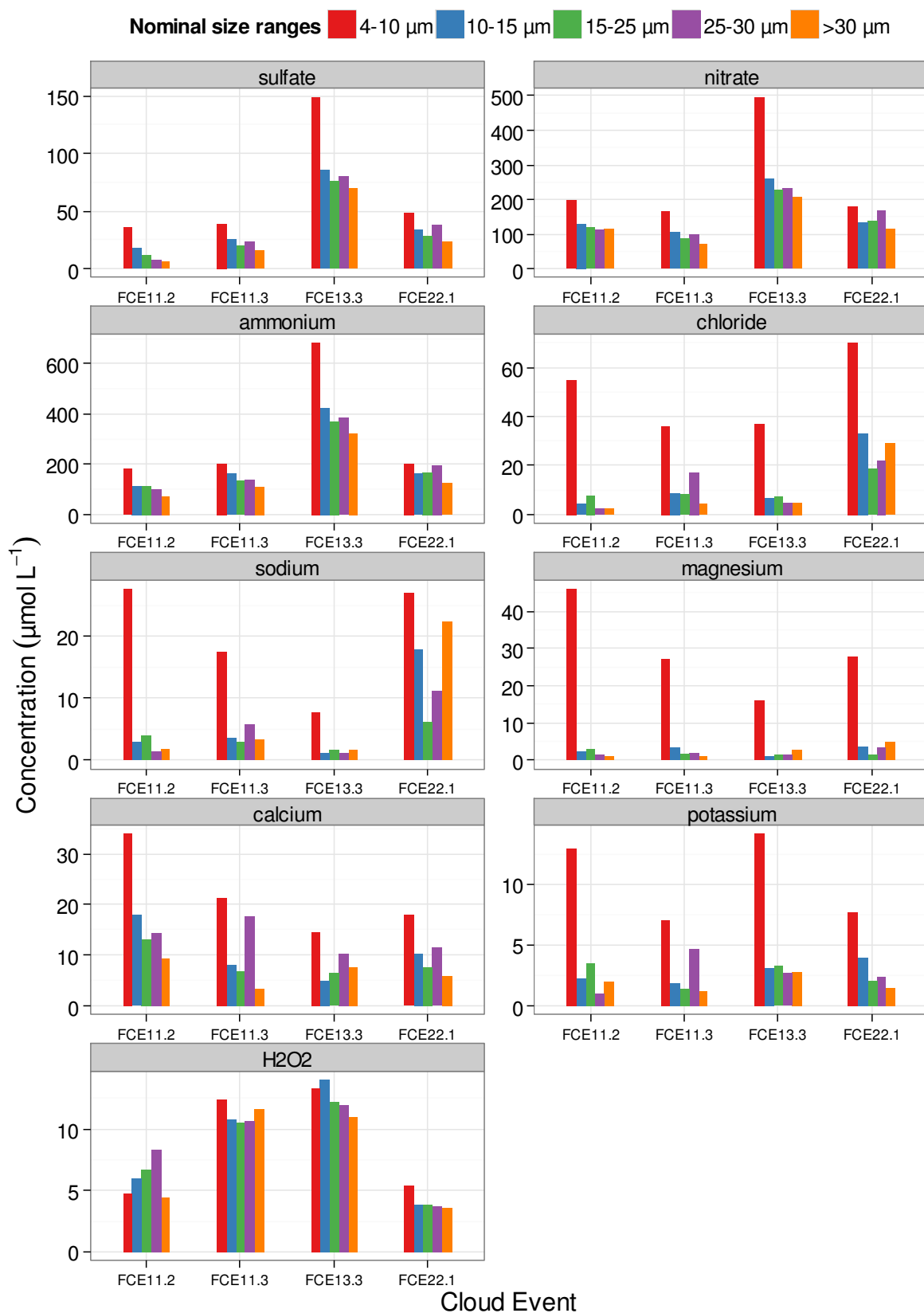


Figure 7: Size-resolved cloud water concentrations from 3-stage collector. Volume-weighted mean concentrations per event are given in  $\mu\text{mol L}^{-1}$  except for DOC ( $\text{mgC L}^{-1}$ ).



**Figure 8: Mean pH values per event, calculated from volume-weighted mean concentrations of  $\text{H}^+$  from (a) 3-stage cloud water collector, and (b) 5-stage collector.**





**Figure 9: Size-resolved cloud water concentrations from 5-stage collector. Volume-weighted mean concentrations per event are given in  $\mu\text{mol L}^{-1}$ .**